Development 130, 1837-1851

doi:10.1242/dev.00400

The role of the zebrafish *nodal*-related genes *squint* and *cyclops* in patterning of mesendoderm

Scott T. Dougan[1,*], Rachel M. Warga[2], Donald A. Kane[2], Alexander F. Schier[3] and William S. Talbot[1,†]

[1]Department of Developmental Biology, Stanford University School of Medicine, Stanford, CA 94305, USA
[2]Department of Biology, University of Rochester, Rochester, NY 14627, USA
[3]Developmental Genetics Program, Skirball Institute of Biomolecular Medicine, Department of Cell Biology, New York University School of Medicine, New York, NY 10016, USA

*Present address: Department of Cellular Biology, University of Georgia, 724 Biological Sciences Building, Athens, GA 30602, USA
†Author for correspondence (e-mail: talbot@cmgm.stanford.edu)

Accepted 9 January 2003

SUMMARY

Nodal signals, a subclass of the TGFβ superfamily of secreted factors, induce formation of mesoderm and endoderm in vertebrate embryos. We have examined the possible dorsoventral and animal-vegetal patterning roles for Nodal signals by using mutations in two zebrafish *nodal*-related genes, *squint* and *cyclops*, to manipulate genetically the levels and timing of Nodal activity. *squint* mutants lack dorsal mesendodermal gene expression at the late blastula stage, and fate mapping and gene expression studies in *sqt*$^{-/-}$; *cyc*$^{+/+}$ and *sqt*$^{-/-}$; *cyc*$^{+/-}$ mutants show that some dorsal marginal cells inappropriately form hindbrain and spinal cord instead of dorsal mesendodermal derivatives. The effects on ventrolateral mesendoderm are less severe, although the endoderm is reduced and muscle precursors are located nearer to the margin than in wild type. Our results support a role for Nodal signals in patterning the mesendoderm along the animal-vegetal axis and indicate that dorsal and ventrolateral mesoderm require different levels of *squint* and *cyclops* function. Dorsal marginal cells were not transformed toward more lateral fates in either *sqt*$^{-/-}$; *cyc*$^{+/-}$ or *sqt*$^{-/-}$; *cyc*$^{+/+}$ embryos, arguing against a role for the graded action of Nodal signals in dorsoventral patterning of the mesendoderm. Differential regulation of the *cyclops* gene in these cells contributes to the different requirements for *nodal*-related gene function in these cells. Dorsal expression of *cyclops* requires Nodal-dependent autoregulation, whereas other factors induce *cyclops* expression in ventrolateral cells. In addition, the differential timing of dorsal mesendoderm induction in *squint* and *cyclops* mutants suggests that dorsal marginal cells can respond to Nodal signals at stages ranging from the mid-blastula through the mid-gastrula.

Key words: Nodal signals, Zebrafish, Spemann organizer, Gastrulation, Dorsoventral axis, Mesoderm

INTRODUCTION

During vertebrate gastrulation, cell movements form three distinct germ layers and elaborate the body axes. In pre-gastrula stage teleost and amphibian embryos, precursors of the three germ layers are distributed at characteristic positions along the animal-vegetal axis. In zebrafish, for example, the cells near the blastoderm margin at the late blastula stage form mesoderm and endoderm (mesendoderm), and are the first to involute at the onset of gastrulation (Kimmel et al., 1990; Warga and Nüsslein-Volhard, 1999). Cells slightly farther from the margin involute at later stages and exclusively become mesodermal cell types. In more animal regions, cells adopt ectodermal fates and do not involute. Each germ layer is patterned along the dorsoventral axis, generating the diverse array of cell types characteristic of the vertebrate body plan. The initial animal-vegetal and dorsoventral asymmetries are established by maternal transcription factors, which regulate zygotic genes controlling cell fate specification and morphogenesis (Harland and Gerhart, 1997; Heasman, 1997; Moon and Kimelman, 1998; Schier and Talbot, 1998; De Robertis et al., 2000; Kimelman and Griffin, 2000; Schier, 2001). Although zygotic factors that can induce and pattern mesoderm have been identified, significant questions remain unanswered about how the mesoderm is patterned.

nodal-related genes encode zygotically acting TGFβ family proteins that are necessary for induction of mesoderm and endoderm (Conlon et al., 1994; Jones et al., 1995; Joseph and Melton, 1997; Schier and Shen, 2000; Takahashi et al., 2000; Schier and Talbot, 2001; Whitman, 2001). Mouse *nodal* mutant embryos lack a primitive streak and fail to form mesodermal derivatives (Conlon et al., 1994; Varlet et al., 1997). In zebrafish, there are two known *nodal*-related genes, *squint* (*sqt*; *ndr1* – Zebrafish Information Network) and *cyclops* (*cyc*; *ndr2* – Zebrafish Information Network) (Erter et al., 1998; Feldman et al., 1998; Rebagliati et al., 1998a; Rebagliati et al., 1998b; Sampath et al., 1998). Whereas defects in *sqt* and *cyc* single

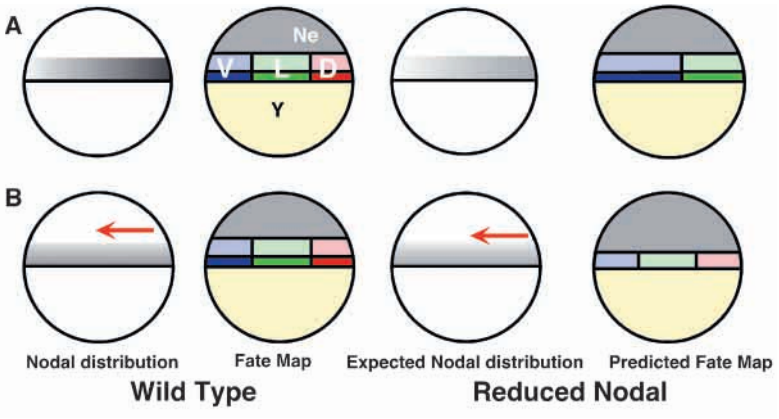

Fig. 1. Two models for the action of Nodal signals in patterning the mesendoderm along the dorsoventral axis in zebrafish embryos. In each case, the gradient of shading at the margin represents the putative distribution of Nodal signals, with the darkest shade indicating the highest concentration. The fate maps shown in the second column are loosely based on those of Kimmel et al. (Kimmel et al., 1990). Mesendoderm is shaded red, green or blue, depending on the position along the dorsoventral axis, and regions generating both mesoderm and endoderm shaded darker than regions producing mesoderm alone. (A) High levels of Nodal signals specify dorsal mesendodermal fates, intermediate levels specify lateral mesendodermal fates and low levels determine ventral mesendoderm. In this model, Nodal signals act in a dorsal-to-ventral gradient to pattern the mesendoderm. The gradient shown here is only one of many such gradients that could be drawn consistent with the evidence. However, all versions of the gradient model predict that reductions in the level of Nodal function would result in the transformation of dorsal marginal cells to more ventrolateral fates (illustrated in the right-hand panels in A). (B) Nodal activity is uniformly distributed along the dorsoventral axis, but a gradient of Nodal signals along the animal-vegetal axis patterns the germ layers. Independent dorsalizing factors pattern the mesendoderm along the dorsoventral axis (represented by the red arrow). This model predicts that endodermal cells (darker colors near the margin) are transformed to more animal fates as levels of Nodal signals are reduced (right-hand panels in B). Dorsalizing factors remain to establish dorsoventral pattern. Ne, neuroectoderm; D, dorsal mesendoderm; L, lateral mesendoderm; V, ventral mesendoderm, Y, yolk.

mutants are largely confined to dorsal axial structures (Hatta et al., 1991; Thisse et al., 1994; Heisenberg and Nüsslein-Volhard, 1997; Feldman et al., 1998; Warga and Nüsslein-Volhard, 1999), almost all mesendodermal derivatives are absent in *sqt; cyc* double mutants, including notochord, trunk somites, pronephros, heart, blood and gut (Feldman et al., 1998). Thus, these *nodal*-related genes have both overlapping and essential functions in mesendoderm development. Cell tracing experiments in *sqt; cyc* double mutants and in maternal-zygotic *one-eyed pinhead* (*oep*) (MZ*oep*) mutants, which are completely unresponsive to Nodal signals (Gritsman et al., 1999), indicate that Nodal signals allocate marginal cells to mesendodermal fates (Feldman et al., 2000; Carmany-Rampey and Schier, 2001).

Although it is now firmly established that Nodal signals induce mesendoderm, a possible role for Nodal signals in specifying different mesendodermal fates along the dorsoventral axis is still controversial. In *Xenopus*, three classes of models have been proposed for the role of activin-like ligands, a group that includes Activin and Nodal signals, in mesoderm patterning (Harland and Gerhart, 1997; Heasman, 1997; McDowell and Gurdon, 1999; De Robertis et al., 2000; Kimelman and Griffin, 2000). One group of models proposes that a gradient of activin-like signals patterns the mesoderm along the dorsoventral axis. This view is supported by explant experiments in which low doses of activin-like signals induced ventrolateral mesodermal fates and high levels induced dorsal fates (Smith et al., 1988; Ruiz i Altaba and Melton, 1989; Green et al., 1992; Agius et al., 2000). Further support for graded action of *nodal*-related genes comes from analysis of the distribution of phosphorylated Smad2, a proposed transcriptional effector of Nodal signals that is initially elevated in the dorsal marginal region in *Xenopus* blastulae (Faure et al., 2000). In addition, Nodal inhibitors block mesoderm formation in different dorsoventral positions in a dosage-dependent manner when overexpressed in *Xenopus* embryos, consistent with asymmetric action of endogenous Nodal signals (Agius et al., 2000).

The second class of models proposes that activin-like signals act uniformly along the dorsoventral axis to induce mesoderm in the marginal region, while independent signals generate dorsoventral pattern (Christian et al., 1992; Kimelman et al., 1992; Clements et al., 1999). This view is supported by experiments with a synthetic activin/TGF-β responsive reporter, which found that the transcriptional output from these signals is uniform along the dorsoventral axis at the beginning of gastrulation (Watabe et al., 1995). Furthermore, promoter analysis indicates that input from both Wnt and activin-like signaling pathways is required for proper expression of dorsal-specific genes, such as *goosecoid* and *siamois* (Watabe et al., 1995; Crease et al., 1998).

Recent work (Lee et al., 2001) supports a third model emphasizing the dynamic action of activin-like signals. The spatiotemporal distribution of phosphorylated Smad2 suggests that these signals are active predominantly in dorsal regions in the late blastula, and that the activity shifts to ventral regions as gastrulation progresses. In addition, activin-like ligands acting in dorsal regions elicit responses at earlier stages than ventrally acting ligands (Lee et al., 2001; Schohl and Fagotto, 2002). These results suggest that dorsoventral patterning involves distinct temporal responses to activin-like signals in dorsal and ventral cells.

Drawing parallels from the work on activin-like signals in *Xenopus*, analysis of Nodal pathway mutants has suggested at least two possible models of Nodal function in zebrafish mesendoderm patterning. The first model proposes graded action of Nodal signals along the dorsoventral axis, with high levels inducing dorsal mesendoderm and low levels inducing ventrolateral mesendoderm (Fig. 1A). In support of this view, dorsal axial structures are reduced in mutants with impaired Nodal signaling, such as *sqt*, *cyc* and *schmalspur* (*sur*) single mutants (Hatta et al., 1991; Heisenberg and Nüsslein-Volhard, 1997; Feldman et al., 1998; Pogoda et al., 2000; Sirotkin et al., 2000a). The expression patterns of *sqt* and *cyc* are consistent with an elevated dorsal requirement for *nodal*-related gene function. Soon after the onset of zygotic

transcription, *sqt* is expressed specifically in the dorsal marginal region, where dorsal mesendoderm originates, and *cyc* is strongly expressed in the axial mesendoderm during gastrulation (Erter et al., 1998; Feldman et al., 1998; Rebagliati et al., 1998a). Moreover, dorsal mesoderm is most sensitive to overexpression of lefty1 (also known as activin), an inhibitor of activin-like signals (Bisgrove et al., 1999; Thisse and Thisse, 1999; Meno et al., 1999; Thisse et al., 2000). Finally, overexpression of high levels of *sqt* or *cyc* induces presumptive ectodermal cells to initiate dorsal mesendodermal gene expression, while lower levels induce pan-mesodermal but not dorsal mesodermal markers (Erter et al., 1998; Sampath et al., 1998; Chen and Schier, 2001). Models in which Nodal activity gradients pattern the dorsoventral axis predict a transformation of cell fates along the dorsoventral axis as Nodal dose is lowered (one scenario is depicted in Fig. 1A, right), but this prediction has not yet been tested by fate-mapping experiments.

The second model proposes that Nodal signals act uniformly along the dorsoventral axis to induce mesendoderm, while independent signals instruct fates along the dorsoventral axis (Fig. 1B). In support of this possibility, dorsoventral asymmetry is established even in the absence of Nodal signals. For example, the dorsal genes *chordin* and *bozozok* (*dharma* – Zebrafish Information Network) are expressed in *sqt; cyc* double mutants and in MZ*oep* mutants (Gritsman et al., 1999; Shimizu et al., 2000; Sirotkin et al., 2000b). The *sqt* and *cyc* genes are expressed uniformly along the dorsoventral margin at the late blastula stage (Erter et al., 1998; Feldman et al., 1998; Rebagliati et al., 1998a; Sampath et al., 1998), consistent with an equivalent requirement in dorsal and ventrolateral regions. Additional evidence derives from the analysis of zygotic *oep* (Z*oep*) mutants (Schier et al., 1997), in which the response to Nodal signals is impaired but not eliminated (Gritsman et al., 1999). Z*oep* mutants lack endodermal derivatives from both the dorsal and ventral margin. Fate mapping of the dorsal marginal region in Z*oep* mutants indicates that the marginal-most cells (prechordal plate precursors) are transformed to a slightly more animal fate (notochord precursors), suggesting that different levels of Nodal signaling distinguish these cell fates (Gritsman et al., 2000). Similarly, low levels of exogenous antivin block endoderm but not mesoderm formation (Thisse and Thisse, 1999; Thisse et al., 2000). If Nodal signals are required uniformly around the margin, reductions in Nodal levels should shift all marginal derivatives toward more animal fates (Fig. 1B, right panels) – a prediction that has not been tested by fate mapping cells in ventrolateral regions.

To test these models and to explore possible stage-specific requirements for *nodal*-related genes, we have assessed mesendodermal patterning and fate specification in $sqt^{-/-}$; $cyc^{+/+}$ and $sqt^{-/-}$; $cyc^{+/-}$ embryos, in which the action of endogenous Nodal signals is reduced but not eliminated. Our results indicate that Nodal signals act in the marginal region to pattern the animal-vegetal axis and that ventrolateral mesendodermal fates can be induced by a lower level of *nodal*-related gene function than dorsal mesendoderm. Furthermore, we find that differential regulation of the *cyclops* gene in dorsal and ventrolateral cells contributes to the different requirements for *nodal*-related gene function in these cells. In addition, our analysis shows that dorsal mesendodermal precursors are competent to respond to Nodal signals over a surprisingly long period, ranging from late blastula through at least early gastrula stages.

MATERIALS AND METHODS

Mutant alleles and photography

$sqt^{cz35}$and $cyc^{m294}$are presumed null alleles that have been described previously (Feldman et al., 1998; Sampath et al., 1998). Embryos were collected from natural crosses and staged as described (Kimmel et al., 1995). Embryos shown in Fig. 4D and Fig. 2A-O were derived from crosses of sqt^{cz35}/+; cyc^{m294}/+ × sqt^{cz35}/+; cyc^{m294}/+ parents. After photography, DNA for genotype analysis was extracted from living embryos as described by Gates et al. (Gates et al., 1999), or from fixed and stained embryos as described by Sirotkin et al. (Sirotkin et al., 2000b). For analysis of *gsc*, embryos with defective *gsc* expression at each stage were counted and a representative sample was photographed; after photography, DNA was extracted for genotyping as previously described. All other mutant embryos, except the *sqt* mutants shown in Fig. 9G-J and Fig. 3E,J were derived from repeated crosses of a small group of sqt^{cz35}/+; cyc^{m294}/+ × sqt^{cz35}/+ parents, in which the majority of sqt^{cz35}/sqt^{cz35}; cyc^{m294}/+ progeny consistently had a truncated notochord and fused somites, as shown in Fig. 2P-U. For quantitation of *foxa2*/*axial* expression at 8 hours post-fertilization (h), stained embryos were photographed as wholemounts in canada balsam: methyl salicylate (11:1), rehydrated in PBT (1× PBS and 0.1% Tween-20), and equilibrated in 80% glycerol. The embryos were then dissected along the ventral midline, photographed under low magnification, and DNA was extracted to determine the genotype by PCR.

Primers and conditions for genotyping sqt^{cz35} and cyc^{m294} have been described (Feldman et al., 1998; Sampath et al., 1998). In crosses with no *cyc* homozygotes, we used a primer pair that amplified a fragment specific to the cyc^{m294} allele to distinguish $cyc^{+/+}$ and cyc^{m294}/+ embryos: forward, 5′-GGTGGACATGCATGTGGATTT-3′ and reverse, 5′-TCGGGCAGGCCCCCTCCCG-3′.

mRNA synthesis and embryo injection

The zβ-catenin expression vector has been described previously (Kelly et al., 1995). Transcripts for injection were synthesized using the Message Machine kit (Ambion). Wild-type embryos were injected with 100 pg *β-catenin* mRNA, while embryos from an intercross of sqt^{cz35}/+ parents were injected with 500 pg *β-catenin* mRNA. In this experiment (Fig. 9G-J), mutant genotypes were inferred from phenotypes rather than assessed by PCR. In the control injection 24% (12/49) of the embryos had reduced *gsc* expression typical of *sqt* mutants (Fig. 9J), whereas the remaining 76% (37/49) displayed normal *gsc* (Fig. 9H). β-catenin overexpression induced ectopic or expanded *gsc* (Fig. 9G) in over half of the wild-type embryos (46/77). β-catenin did not induce high levels of *gsc* expression in *sqt* mutants, because 26% (16/62) of injected embryos displayed reduced *gsc* typical of uninjected *sqt* mutants (Fig. 9I).

Immunocytochemistry and in situ hybridization

For analysis of the distribution of β-catenin protein, wild-type embryos were fixed at 15 minute intervals during the first 4 hours of embryogenesis, processed for immunocytochemistry with β-catenin antibodies and sectioned. Polyclonal anti-β-catenin antibodies (Schneider et al., 1996) were used at a 1:1000 dilution. Immunostaining was carried out as described (Schier et al., 1997). For sectioning, embryos were embedded in Eponate-12 resin and sectioned at 3 μm. Twenty embryos were analyzed at each time-point, and two or three of these were sectioned to confirm the presence or absence of nuclear β-catenin. Although the majority of embryos after the 1000-cell stage exhibited β-catenin protein in dorsal nuclei (in both

Table 1. Phenotypes of *sqt*$^{-/-}$, *cyc*$^{-/-}$, *sqt*$^{-/-}$; *cyc*$^{+/-}$ and *sqt*$^{-/-}$; *cyc*$^{-/-}$ mutants

Parental genotype	Mutant genotype	Total number of mutants	Number with normal shields at 6 h	Number with two eyes at 1 d	Number with swim bladder at 5 d	Number with fused somites at 12 h	Number with Kupffer's vesicle at 12 h
cyc$^{+/-}$	*cyc*$^{-/-}$	32	32	0	0	nd	nd
sqt$^{+/-}$	*sqt*$^{-/-}$	24	0	22	18	nd	nd
sqt$^{+/-}$;*cyc*$^{+/-}$	*sqt*$^{+/+}$; *cyc*$^{-/-}$ or *sqt*$^{+/-}$; *cyc*$^{-/-}$	18	18	0	0	nd	nd
	sqt$^{-/-}$; *cyc*$^{+/+}$	9	0	9	8	nd	nd
	sqt$^{-/-}$; *cyc*$^{+/-}$	10	0	1	1	nd	nd
	sqt$^{-/-}$; *cyc*$^{-/-}$	7	0	0	nd	nd	nd
sqt$^{+/-}$;*cyc*$^{+/-}$ × *sqt*$^{+/-}$;*cyc*$^{+/+}$	*sqt*$^{-/-}$; *cyc*$^{+/+}$	12	nd	nd	nd	3	0
	sqt$^{-/-}$; *cyc*$^{+/-}$	11	nd	nd	nd	7	0

nd, not determined; h, hours post-fertilization; d, days post-fertilization.

the YSL and blastomeres), only three embryos at the 128-cell stage, three embryos at the 256-cell stage and three embryos at the 512 stage exhibited β-catenin protein in dorsal nuclei. At all stages, staining of membrane localized β-catenin protein served as a positive control for the antibody reaction.

Synthesis of probes and in situ hybridization were conducted as described (Sirotkin et al., 2000b). After in situ hybridization, the number of mutant embryos from each cross was counted and representative examples of each phenotype were photographed and genotyped by PCR, except when the genotype could be inferred from morphology as in the analysis of *gsc* at 10 h in *sqt*$^{-/-}$; *cyc*$^{+/-}$ and *sqt*$^{-/-}$; *cyc*$^{-/-}$ embryos and *sox17* expression in *sqt*$^{-/-}$; *cyc*$^{+/-}$ mutants. The number of mutants was usually close to the expected values, and the same mutant phenotypes were observed in repeated crosses of the same parents.

Lineage-tracing and fate map analysis

Embryos of *sqt*^{cz35}/+; *cyc*^{m294}/+ × *sqt*^{cz35}/+ parents were injected (Kimmel et al., 1990) with the lineage tracer dye tetramethylrhodamine-isocyanate dextran (Molecular Probes, Eugene, OR; 10×10^3 M_r, diluted to 5% (wt/vol) in 0.2 M KCl) in single blastomeres of the surface enveloping layer (EVL) at the 1000-cell stage. Injected embryos were mounted in 0.125% agarose in embryo medium and oriented so that the fluorescent cells faced toward the microscope objective; the position of the clone along the animal-vegetal axis was then determined. The clonal position relative to the dorsoventral axis was determined at 6 h, when the dorsal side is first morphologically apparent in wild-type embryos, or at 8 h, when the dorsal side is morphologically apparent in *sqt*$^{-/-}$; *cyc*$^{+/-}$ embryos. Some embryos were filmed during gastrulation with time-lapse photography as previously described (Warga and Kimmel, 1990). After filming, embryos were removed from agarose and the fates of the resulting clones were determined at 24 h and 48 h, after which all embryos were genotyped by PCR.

RESULTS

Genetic interaction between *nodal*-related genes reveals dosage-sensitive function of *cyclops*

To understand the role of Nodal signaling in patterning the mesendoderm, we analyzed the phenotypes of embryos with reduced *nodal* gene function, including *sqt*$^{-/-}$; *cyc*$^{+/+}$ and *sqt*$^{-/-}$; *cyc*$^{+/-}$ mutants. At 6 h, *sqt*$^{-/-}$; *cyc*$^{+/+}$ single mutants lack a morphologically visible embryonic shield, the site of presumptive dorsal mesendoderm (Table 1) (Feldman et al., 1998). Kupffer's vesicle, a derivative of the dorsal forerunner cells (Cooper and D'Amico, 1996; Melby et al., 1996), was reduced or absent at 12 h (Fig. 2T). Forerunner cells were also reduced or absent in *sqt*$^{-/-}$; *cyc*$^{+/+}$ mutants (see Fig. 5J-L, arrows), as revealed by expression of *sox17* (Alexander and Stainier, 1999). Thus, most or all *sqt*$^{-/-}$; *cyc*$^{+/+}$ single mutants have defects in dorsal marginal structures at the onset of gastrulation. At 24 h, a variable fraction of *sqt* mutants display mild cyclopia and reduction of ventral diencephalon (Table 1; Fig. 2I) and some *sqt*$^{-/-}$; *cyc*$^{+/+}$ single mutants are morphologically indistinguishable from wild type (Table 1; data not shown). The amelioration of the *sqt* mutant phenotype at later stages depends on the function of *cyc*, because *sqt; cyc* double mutants lack all mesendodermal derivatives in the head and trunk at 24 h (Fig. 2A-C) (Feldman et al., 1998).

To search for possible dosage-sensitive functions for *squint* and *cyclops*, we compared the phenotypes of *sqt*$^{-/-}$; *cyc*$^{+/+}$ and *sqt*$^{-/-}$; *cyc*$^{+/-}$ embryos, which differ by a single copy of *cyc*. Like *sqt*$^{-/-}$; *cyc*$^{+/+}$ single mutants, *sqt*$^{-/-}$; *cyc*$^{+/-}$ embryos did not form an embryonic shield or Kupffer's vesicle (Table 1; Fig. 2U). At later stages, however, *sqt*$^{-/-}$; *cyc*$^{+/-}$ embryos had a significantly stronger phenotype than *sqt*$^{-/-}$; *cyc*$^{+/+}$ embryos (Fig. 2, compare D-F to G-I). For example, the notochord was severely reduced or truncated in most *sqt*$^{-/-}$; *cyc*$^{+/-}$ embryos (Fig. 2E), although it formed normally in the majority of *sqt*$^{-/-}$; *cyc*$^{+/+}$ single mutants (Fig. 2H). In *sqt*$^{-/-}$; *cyc*$^{+/-}$ embryos with truncated notochords, the somites were often fused across the midline (Fig. 2R), as were adaxial and paraxial domains of *myod* expression (Weinberg et al., 1996) (Fig. 6A-F). In addition, *sqt*$^{-/-}$; *cyc*$^{+/-}$ embryos have more pronounced cyclopia than *sqt*$^{-/-}$; *cyc*$^{+/+}$ embryos (Fig. 2F,I), suggesting a greater reduction in prechordal plate mesoderm. The severity of these defects varies with the genetic background, but within a group of siblings the typical *sqt*$^{-/-}$; *cyc*$^{+/-}$ embryo has a stronger phenotype than the typical *sqt*$^{-/-}$; *cyc*$^{+/+}$ sibling. These results indicate that the formation of dorsal axial structures in *sqt* mutants is strongly dependent on *cyc* gene dosage, such that the phenotype of *sqt*$^{-/-}$; *cyc*$^{+/+}$ embryos is compounded by the loss of a single copy of *cyc* (i.e. in *sqt*$^{-/-}$; *cyc*$^{+/-}$ embryos). Conversely, we did not note any differences between the phenotypes of *sqt*$^{+/+}$; *cyc*$^{-/-}$ and *sqt*$^{+/-}$; *cyc*$^{-/-}$ embryos (Fig. 2J-L; Table 1; data not shown).

Dorsal expression of *cyc* is activated by *sqt* and by autoregulation

Maintenance of *sqt* and *cyc* expression depends on the ability of cells to respond to Nodal signaling (Meno et al., 1999;

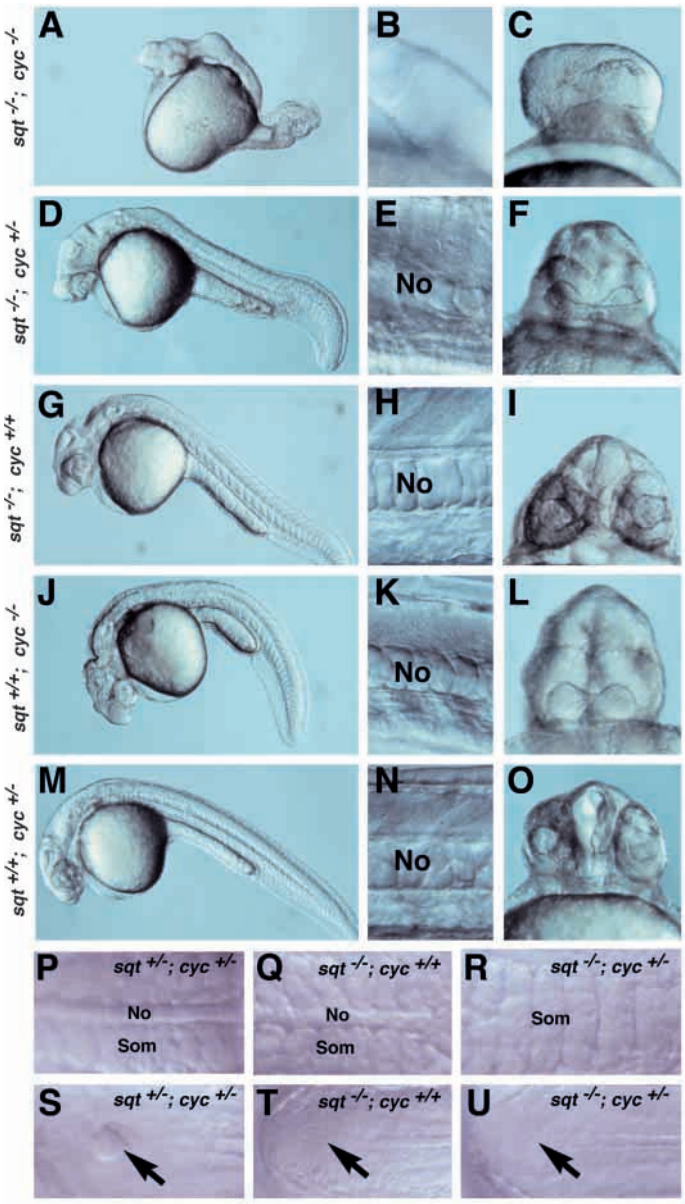

Fig. 2. Analysis of genetic interaction between *sqt* and *cyc*. Images of 28 hour embryos from a *sqt*$^{+/-}$; *cyc*$^{+/-}$ intercross (A-O) or cross of *sqt*$^{+/-}$; *cyc*$^{+/-}$ to *sqt*$^{+/-}$; *cyc*$^{+/+}$ parents (P-U). Phenotypes were scored at 6 h, 1 d and 5 d; an embryo representative of each phenotypic class is shown. (A-C) *sqt*$^{-/-}$; *cyc*$^{-/-}$ embryos lack head and trunk mesoderm and endoderm derivatives, and display severe cyclopia (C). Tail mesoderm still forms in these embryos, as indicated by the presence of tail somites (A). (D-F) Trunk somites, heart and blood form in *sqt*$^{-/-}$; *cyc* $^{+/-}$ embryos (D). These embryos have strong midline defects, including a reduced notochord and missing floor plate (E) as well as cyclopia (F), which is indicative of defects in prechordal plate mesoderm. These defects are typically more severe than those observed in sibling *sqt*$^{-/-}$; *cyc* $^{+/+}$ embryos (G-I), which are often indistinguishable from wild type (M-O), and can survive to adulthood. Some *sqt*$^{-/-}$; *cyc* $^{+/+}$ embryos display mild cyclopia (I), but have normal notochords and floor plates. (J-L) The defects in *sqt*$^{+/+}$; *cyc*$^{-/-}$ embryos include a curved body axis (J), missing floor plate (K) and cyclopia (L); these embryos have apparently normal trunk somites and notochord (K). In other clutches, the majority of *sqt*$^{-/-}$; *cyc*$^{+/-}$ embryos have truncated notochords and fused somites (R), unlike typical *sqt*$^{-/-}$; *cyc*$^{+/+}$ siblings (Q). Kupffer's vesicle is apparent in the tailbuds of 12-14 h wild-type embryos (S, arrow), but is reduced or absent in *sqt*$^{-/-}$; *cyc* $^{+/+}$ and *sqt*$^{+/+}$; *cyc*$^{-/-}$ embryos (T,U, arrows). Anterior is towards the left in A-R, except for head views in C,F,I,L,O. Posterior is towards the left in S-U. No, notochord; Som, somites. The genotypes of all embryos shown were determined by PCR after photography.

Pogoda et al., 2000; Sirotkin et al., 2000a). Therefore we investigated the role of crossregulation in the dosage-sensitive interaction between *sqt* and *cyc* by examining *cyc* expression in *sqt* mutants and *sqt* expression in *cyc* mutants. Expression of *sqt* appeared normal in a time course of *cyc* mutant embryos (compare Fig. 3F-I with 3A-D), but was reduced in *sqt* mutants (Fig. 3E,J). *cyc* expression was altered in *sqt*$^{-/-}$; *cyc*$^{+/+}$ mutants (compare Fig. 3L-O with 3P-S). Although *cyc* expression initiated in *sqt* mutants (Fig. 3P), it was reduced or absent at the dorsal margin at 5 h (Fig. 3Q) and was evident at the dorsal midline at reduced levels during gastrulation (Fig. 3R,S). Expression of *cyc* was reduced significantly in *sqt*$^{-/-}$; *cyc*$^{+/-}$ mutants (Fig. 3T-V) in comparison with *sqt*$^{-/-}$; *cyc*$^{+/+}$ embryos (Fig. 3Q-S). At the onset of gastrulation in *sqt*$^{-/-}$; *cyc*$^{+/-}$ mutants, *cyc* transcripts were present in only two weak dorsolateral patches (Fig. 3U); the dorsal gap between these patches closed as gastrulation progressed, such that a narrow strip of *cyc* expression was visible at the dorsal midline at 8 h (Fig. 3V). These results show that dorsal *cyc* expression is activated by *sqt* at 5 h, the first stage where a reduction of *cyc* expression is evident in *sqt* mutants. The reduction of *cyc* expression in *sqt*$^{-/-}$; *cyc*$^{+/-}$ embryos when compared with *sqt*$^{-/-}$; *cyc*$^{+/+}$ mutants suggests that *cyc* expression also activates its own transcription. It is not likely that a reduction of mutant mRNA stability is the cause of reduced *cyc* expression in *sqt*$^{-/-}$; *cyc*$^{+/-}$ mutants, because the level and pattern of *cyc* mRNA expression was not altered in *sqt*$^{+/+}$; *cyc*$^{+/-}$ embryos when compared with wild type (data not shown).

Mesendoderm induction requires different levels of *nodal*-related gene function in dorsal and ventrolateral regions

To examine the effect of reduced Nodal signaling on dorsoventral patterning of the mesendoderm, we analyzed the time course of expression of an array of marker genes in *sqt*$^{-/-}$; *cyc*$^{+/+}$ and *sqt*$^{-/-}$; *cyc*$^{+/-}$ mutants. For these experiments, we analyzed clutches of embryos in which most *sqt*$^{-/-}$; *cyc*$^{+/-}$ mutants had strong cyclopia, truncated notochords, and medially fused somites. Embryos from appropriate crosses were harvested at blastula and gastrula stages, analyzed by whole-mount in situ hybridization, assigned to phenotypic classes based on expression patterns, and then genotyped by PCR assays to determine which genotypes constituted each phenotypic class. As expected from morphological analysis, markers for dorsal mesendoderm such as *gsc* and *axial/foxa2* were reduced more severely in *sqt*$^{-/-}$; *cyc*$^{+/-}$ embryos than in *sqt*$^{-/-}$; *cyc*$^{+/+}$ single mutants. Expression of *gsc*, which marks the prechordal plate during gastrulation (Stachel et al., 1993), initiated in the dorsal marginal region in *sqt*$^{-/-}$; *cyc*$^{+/+}$, *sqt*$^{-/-}$; *cyc*$^{+/-}$ and *sqt*$^{-/-}$; *cyc*$^{-/-}$ embryos (Fig. 4B1,C1,D1), but it rapidly faded in embryos of all three mutant genotypes (Fig.

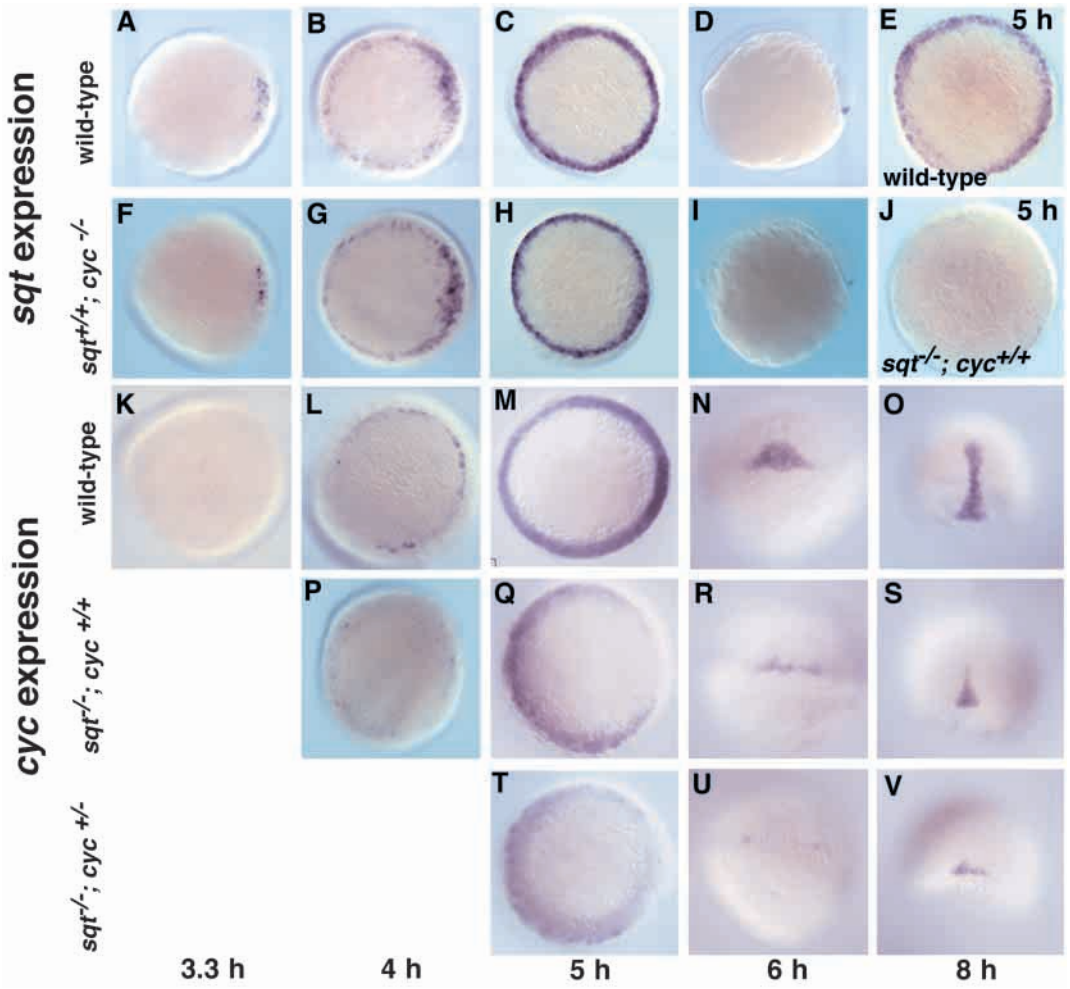

Fig. 3. Analysis of crossregulation between *squint* and *cyclops*. Time course of *sqt* expression in wild-type (A-E), *sqt* mutant (J) and *cyc* mutant embryos (F-I). *cyc* expression in wild-type (K-O), $sqt^{-/-}$; $cyc^{+/+}$ (P-S) and $sqt^{-/-}$; $cyc^{+/-}$ (T-V) embryos. Developmental stages are indicated at the bottom, except for E and J, which are 5 h embryos as noted in the panels. Although the absence of *sqt* transcripts in *sqt* mutants is consistent with an autoregulatory role for *sqt*, it is also possible that the 1.9 kb insertion in the sqt^{cz35} allele affects the stability of the message. Animal pole views are shown for all embryos prior to 6 h, and dorsal views are shown for embryos at 6 and 8 h, except for the lateral images in D,I. The genotypes of all embryos shown were determined by PCR after photography, except for E and J, for which the genotypes were inferred from the phenotypic ratio evident in progeny from a *sqt*/+ intercross (10 mutants/33 progeny).

4B2,C2,D2). By 5 h (40% epiboly), *gsc* transcripts were prominent at the dorsal margin of wild-type embryos (Fig. 4A2), but were detectable in only a few cells in $sqt^{-/-}$; $cyc^{+/+}$ mutants (Fig. 4B2). We were unable to detect *gsc* expression in $sqt^{-/-}$; $cyc^{+/-}$ and $sqt^{-/-}$; $cyc^{-/-}$ embryos at this stage (Fig. 4C2,D2). *gsc* expression recovered during gastrulation in $sqt^{-/-}$; $cyc^{+/+}$ mutants (Fig. 4B3-B6), but not in $sqt^{-/-}$; $cyc^{+/-}$ and $sqt^{-/-}$; $cyc^{-/-}$ mutant siblings (Fig. 4C3-C5,D3-D5). After gastrulation, weak ectodermal *gsc* expression initiated in both $sqt^{-/-}$; $cyc^{+/-}$ and $sqt^{-/-}$; $cyc^{-/-}$ mutants (Fig. 4C6,D6). Like *gsc*, expression of *axial/foxa2* in axial mesoderm (Strähle et al., 1993) is reduced to a much greater extent in $sqt^{-/-}$; $cyc^{+/-}$ embryos than $sqt^{-/-}$; $cyc^{+/+}$ siblings (Fig. 5A-F). And like *gsc*, *axial/foxa2* expression at the midline later recovers in $sqt^{-/-}$; $cyc^{+/+}$ embryos (data not shown). Thus, early dorsal mesendodermal gene expression is reduced in $sqt^{-/-}$; $cyc^{+/+}$ single mutants, and the further loss of a single copy of the *cyclops* gene compounds this defect. The recovery of dorsal mesoderm gene expression in some *sqt* mutants suggests that dorsal marginal cells can adopt dorsal mesendoderm fates in response to *cyc* signaling during gastrulation, more than 2 hours after dorsal mesendoderm induction occurs in wild type.

To examine how the endoderm is affected in $sqt^{-/-}$; $cyc^{+/+}$ and $sqt^{-/-}$; $cyc^{+/-}$ mutants embryos, we analyzed expression of *axial/foxa2* and *sox17* (Fig. 5A-L) (Schier et al., 1997; Alexander and Stainier, 1999). In order to quantify endodermal progenitors, we made fillets of mid-gastrula stage wild-type and mutant embryos stained for *axial/foxa2* expression and counted the total number of labeled endodermal cells (Fig. 5M). At mid-gastrulation, wild-type embryos (n=4) had an average of 270 (±54) *axial/foxa2*-expressing endodermal cells, $sqt^{-/-}$; $cyc^{+/+}$ embryos (n=5) had an average of 164 (±35), and $sqt^{-/-}$; $cyc^{+/-}$ embryos (n=5) had only 65 (±12). A similar distribution of endodermal cells was observed in $sqt^{-/-}$; $cyc^{+/+}$ and $sqt^{-/-}$; $cyc^{+/-}$ mutants at 10 h and 12 h, as detected by *sox17* expression (data not shown). The reduction in endodermal precursors was not uniform along the dorsoventral axis (Fig. 5N). In wild-type embryos, previous work showed that endoderm is asymmetrically distributed at mid-gastrulation (Warga and Nüsslein-Volhard, 1999), and we found an average of 13 rows of *axial/foxa2*-expressing endodermal cells dorsally, compared with only four rows ventrally (Fig. 5N). This asymmetry was less pronounced in $sqt^{-/-}$; $cyc^{+/+}$ embryos, which had an average of only seven tiers of axial-expressing cells dorsally and 2.5 tiers ventrally. Dorsal endoderm was completely eliminated in $sqt^{-/-}$; $cyc^{+/-}$ embryos, although one to three tiers of *axial/foxa2*-expressing cells remained ventrally and laterally. Thus, like mesoderm, endoderm in dorsal locations in *sqt* mutants is more sensitive to reductions in *cyc* gene dosage than endoderm in lateral and ventral positions.

We next investigated whether the loss of dorsal

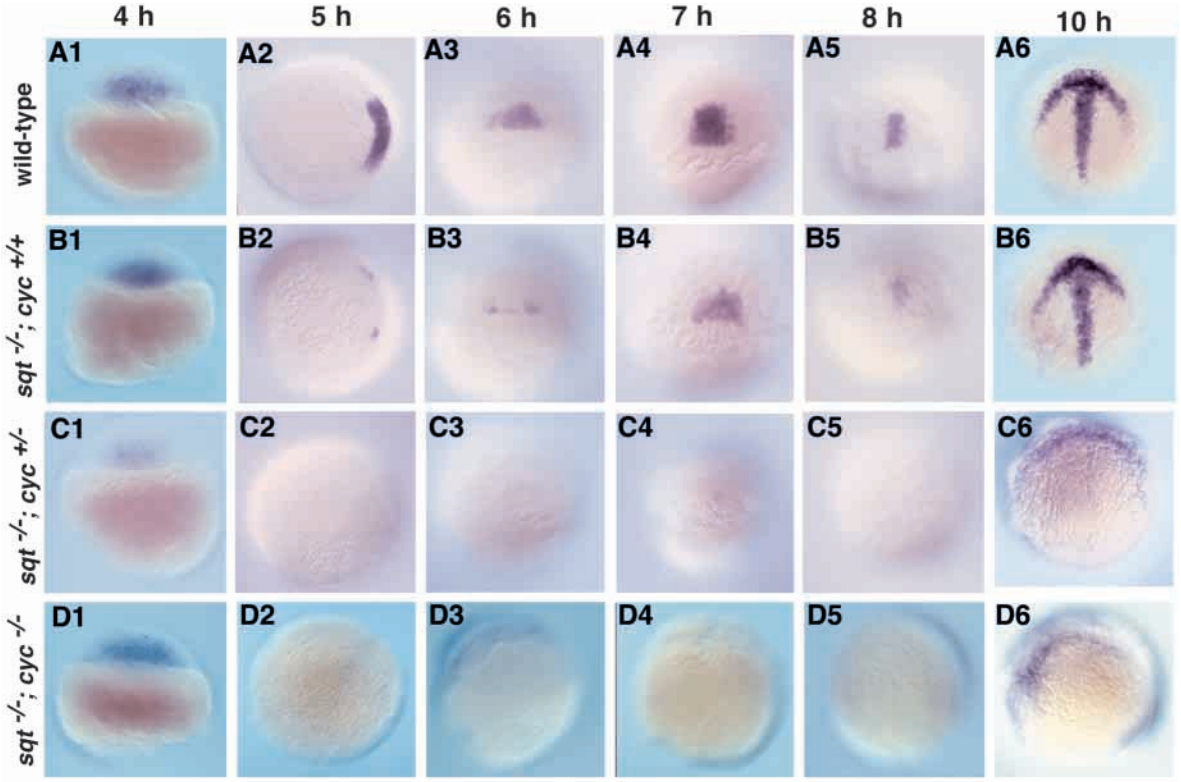

Fig. 4. Time course of dorsal mesendoderm development in *sqt*$^{-/-}$; *cyc*$^{+/+}$, *sqt*$^{-/-}$; *cyc*$^{+/-}$ and *sqt*$^{-/-}$; *cyc*$^{-/-}$ mutants. *gsc* expression in wild-type (A), *sqt*$^{-/-}$; *cyc*$^{+/+}$(B), *sqt*$^{-/-}$; *cyc*$^{+/-}$(C) and *sqt*$^{-/-}$; *cyc*$^{-/-}$ (D) embryos . For each stage, wild-type, *sqt*$^{-/-}$; *cyc*$^{+/+}$, *sqt*$^{-/-}$; *cyc*$^{+/-}$ are siblings; the *sqt*$^{-/-}$; *cyc*$^{-/-}$, mutants were derived from a separate cross that was processed in parallel. The images for panels C6 and D6 come from a separate cross of *sqt*$^{+/-}$; *cyc*$^{+/-}$ adults. *gsc* expression initiates in *sqt*$^{-/-}$; *cyc*$^{+/+}$, *sqt*$^{-/-}$; *cyc*$^{+/-}$ and *sqt*$^{-/-}$; *cyc*$^{-/-}$ embryos (A1,B1,C1,D1), but is rapidly lost (B2,C2,D2). In *sqt*$^{-/-}$; *cyc*$^{+/+}$ embryos, *gsc* is expressed only in a few cells at 5 h, but steadily increases throughout gastrulation such that it is often indistinguishable from wild-type at bud stage (B2-B6). Dorsal views are shown, except for animal views at 5 and 10 h. The genotypes of all embryos shown were determined by PCR after photography, except for panels C6 and D6, which were determined by morphology. In the *sqt*$^{+/-}$; *cyc*$^{+/+}$ intercross depicted in A6, B6, only 3/51 embryos displayed reduced *gsc* expression; the rest of the embryos, including the remaining *sqt* mutants, have a wild-type pattern as shown. Notably, we found no reduction of *gsc* expression in *cyc*^{m294} homozygotes at 8 h (data not shown). This contrasts with earlier work on *cyc*^{b16} (Thisse et al., 1994), which is now known to be a deficiency that removes other genes in the *cyclops* region of linkage group 12 (Talbot et al., 1998).

mesendodermal markers is accompanied by a corresponding alteration in ventrolateral gene expression (Fig. 6). The ventrolateral mesoderm markers *spadetail* (*spt*; *tbx16* – Zebrafish Information Network), *tbx6* and *vox* (Hug et al., 1997; Griffin et al., 1998; Kawahara et al., 2000; Melby et al., 2000) are each expressed around the margin but are largely excluded from dorsal marginal regions (Fig. 6G,J,M,P). Ventrolateral expression of these genes was not significantly altered in *sqt*$^{-/-}$; *cyc*$^{+/+}$ or *sqt*$^{-/-}$; *cyc*$^{+/-}$ mutant embryos (Fig. 6H,K,N,Q), except that each of these genes was excluded from a larger dorsal sector in *sqt*$^{-/-}$; *cyc*$^{+/-}$ embryos (Fig. 6I,L,O,R). The different effects on dorsal and ventrolateral mesendodermal gene expression in *sqt*$^{-/-}$; *cyc*$^{+/+}$ and *sqt*$^{-/-}$; *cyc*$^{+/-}$ mutants suggests that the formation of mesoderm and endoderm requires higher levels of *cyc* function at the dorsal margin than at the ventrolateral margin.

Dorsal marginal cells adopt neural fates in *sqt*$^{-/-}$; *cyc*$^{+/+}$ and *sqt*$^{-/-}$; *cyc*$^{+/-}$ mutants

As dorsal marginal cells fail to express markers for both dorsal and ventrolateral mesendoderm in *sqt*$^{-/-}$; *cyc*$^{+/-}$ mutants, we wished to determine the fates of dorsal marginal cells in these embryos. Expression of the pan-mesodermal marker *ntl/brachyury* (Schulte-Merker et al., 1992), was reduced on the dorsal side of *sqt*$^{-/-}$; *cyc*$^{+/+}$ embryos (Fig. 6T) and absent from a dorsal sector in *sqt*$^{-/-}$; *cyc*$^{+/-}$ embryos (Fig. 6U), raising the possibility that dorsal marginal cells adopt a neurectodermal fate in *sqt*$^{-/-}$; *cyc*$^{+/-}$ mutants. Accordingly, the neural plate marker *cyp26* (White et al., 1996; Thisse and Thisse, 1999; Kudoh et al., 2001) was positioned closer to the margin in *sqt*$^{-/-}$; *cyc*$^{+/+}$ and *sqt*$^{-/-}$; *cyc*$^{+/-}$ mutants than in wild type (Fig. 6W,X, arrowheads).

The gene expression studies prompted us to determine directly the fates of marginal cells in *sqt*$^{-/-}$; *cyc*$^{+/+}$ and *sqt*$^{-/-}$; *cyc*$^{+/-}$ mutants. We labeled single blastomeres at the 1000-cell stage by injection of a lineage tracer dye and ascertained the fates of their progeny between 1 and 3 d, when most cells have differentiated. Dorsal cells closest to the margin in wild-type embryos exclusively form mesodermal and endodermal derivatives, including hatching gland, foregut and notochord (Kimmel et al., 1990; Melby et al., 1996; Warga and Nüsslein-Volhard, 1999). By contrast, some dorsal marginal cells in *sqt*$^{-/-}$; *cyc*$^{+/+}$ and *sqt*$^{-/-}$; *cyc*$^{+/-}$ mutants adopt neural fates, including spinal cord, hindbrain and midbrain (Fig. 7B,C,

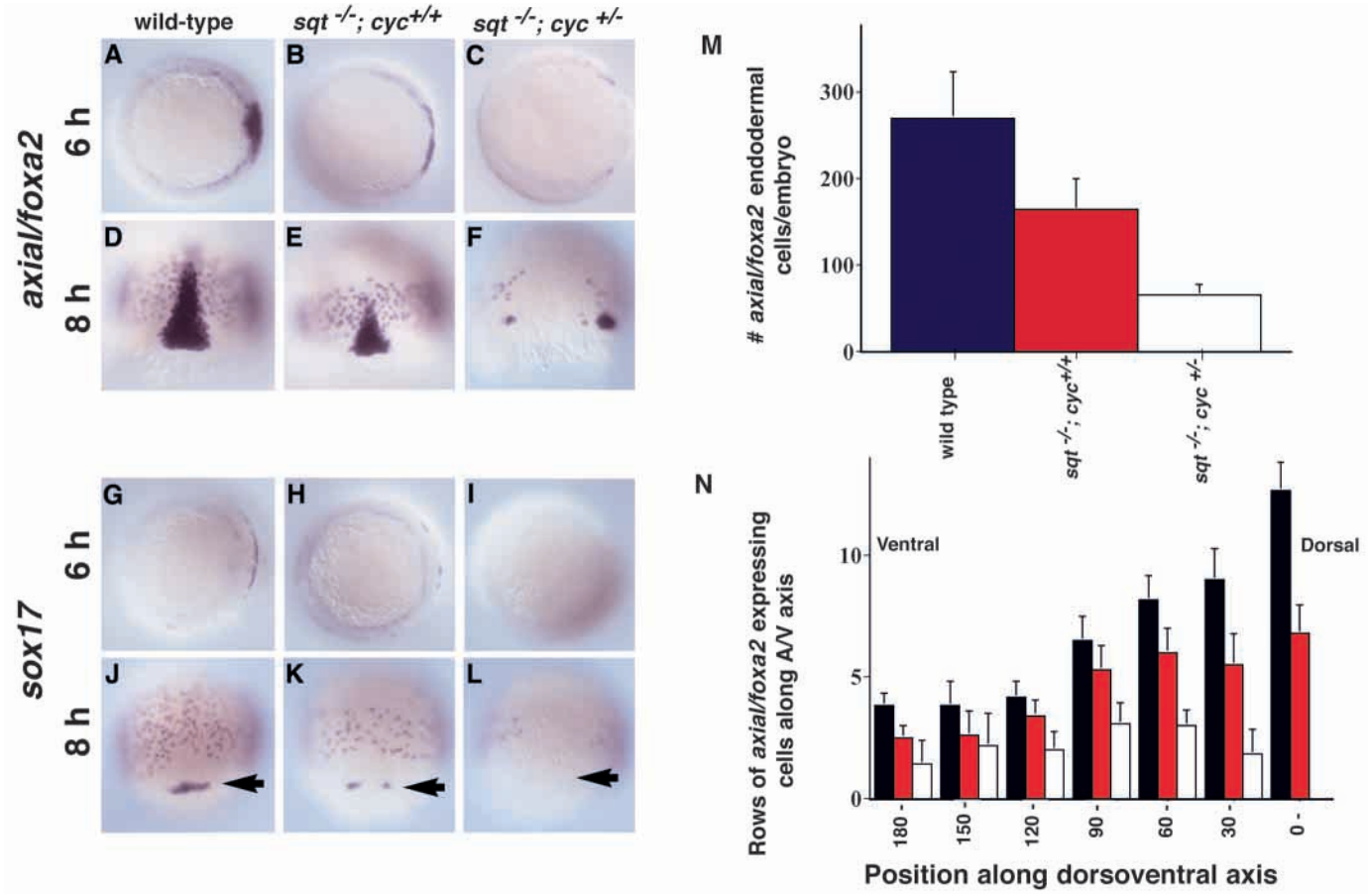

Fig. 5. Endoderm development in *sqt*$^{-/-}$; *cyc*$^{+/+}$ and *sqt*$^{-/-}$; *cyc*$^{+/-}$ mutants. Expression of *axial/foxa2* (A-F) or *sox17* (G-L) in wild-type (A,D,G,J), *sqt*$^{-/-}$; *cyc*$^{+/+}$ (B,E,H,K) and *sqt*$^{-/-}$; *cyc*$^{+/-}$ (C,F,I,L) embryos at 6 h (A-C,G-I; animal pole views) and 8 h (D-F,J-L; dorsal views). The reduction of endodermal expression of *axial/foxa2* and *sox17* in *sqt*$^{-/-}$; *cyc*$^{+/+}$ and *sqt*$^{-/-}$; *cyc*$^{+/-}$ embryos is particularly apparent on the dorsal margin (E,F,K,L). Arrows in J-L indicate the position of dorsal forerunner cells. (M) The total number of endodermal precursors expressing *axial/foxa2* at 8 h in wild-type embryos (n=3), *sqt*$^{-/-}$; *cyc*$^{+/+}$ embryos (n=4) and *sqt*$^{-/-}$; *cyc*$^{+/-}$ embryos (n=5). (N) Reduction of *axial/foxa2* expressing endodermal cells at different positions along the dorsoventral axis (dorsal midline set at zero degrees, ventral midline at 180 degrees). Height of each bar indicates the number of marginal cell tiers along the animal-vegetal axis expressing *axial/foxa2*. No cells at the dorsal midline expressed *axial/foxa2* in *sqt*$^{-/-}$; *cyc*$^{+/-}$ embryos. The genotype is indicated by color, as shown in M. The genotypes of all embryos shown were determined by PCR after photography.

upper panels), which derive from more animal regions in wild-type embryos (Fig. 7A). In two cases, mutant dorsal marginal clones exclusively generated neural fates (*sqt*$^{-/-}$; *cyc*$^{+/+}$ n=1; *sqt*$^{-/-}$; *cyc*$^{+/-}$ n=1), which is never observed in wild type. In addition, dorsal marginal cells formed foregut endoderm and hatching gland rarely if at all in *sqt*$^{-/-}$; *cyc*$^{+/+}$ and *sqt*$^{-/-}$; *cyc*$^{+/-}$ mutants, although these cells can form notochord. As previously reported (Feldman et al., 2000; Carmany-Rampey and Schier, 2001), all dorsal marginal cells adopt neural fates in the absence of Nodal signaling (Fig. 7D).

In none of these experiments did we find evidence that disruption of *nodal*-related genes shifted the fates of dorsal marginal cells along the dorsoventral axis. There was instead clear evidence that marginal cells adopt fates characteristic of more animal positions. This animal-vegetal fate shift was most apparent at the dorsal margin, where cells adopt neural fates in *sqt*$^{-/-}$; *cyc*$^{+/+}$ and *sqt*$^{-/-}$; *cyc*$^{+/-}$ mutants (Fig. 7B,C, upper panels). There is also evidence to suggest an animal-vegetal fate shift at the ventrolateral margin, where muscle precursors are located closer to the margin than in wild type (Fig. 7B,C, middle panels).

Abnormal morphogenesis of dorsal marginal cells in *sqt*$^{-/-}$; *cyc*$^{+/-}$ mutants

In addition to changes in cell fate, we observed that dorsal marginal cells undergo an aberrant morphogenetic behavior in *sqt*$^{-/-}$; *cyc*$^{+/-}$ embryos, consistent with their altered cell fates (Fig. 7 and Fig. 8B). At the onset of gastrulation, dorsal marginal cells enter the mesendodermal germ layer and rapidly move toward the animal pole, forming the prechordal plate (n=16 clones, Fig. 8A) (Warga and Nüsslein-Volhard, 1999). Instead of undergoing normal involution movements and moving toward the animal pole, dorsal marginal cells in *sqt*$^{-/-}$; *cyc*$^{+/-}$ embryos dispersed along the margin. Many dorsal cells in mutants rolled inwards, temporarily altered their course and then continued migrating toward the vegetal pole (Fig. 8B, n=3 clones in *sqt*$^{-/-}$; *cyc*$^{+/-}$ embryos). Despite their anomalous behavior, some of these dorsal cells were able to contribute to

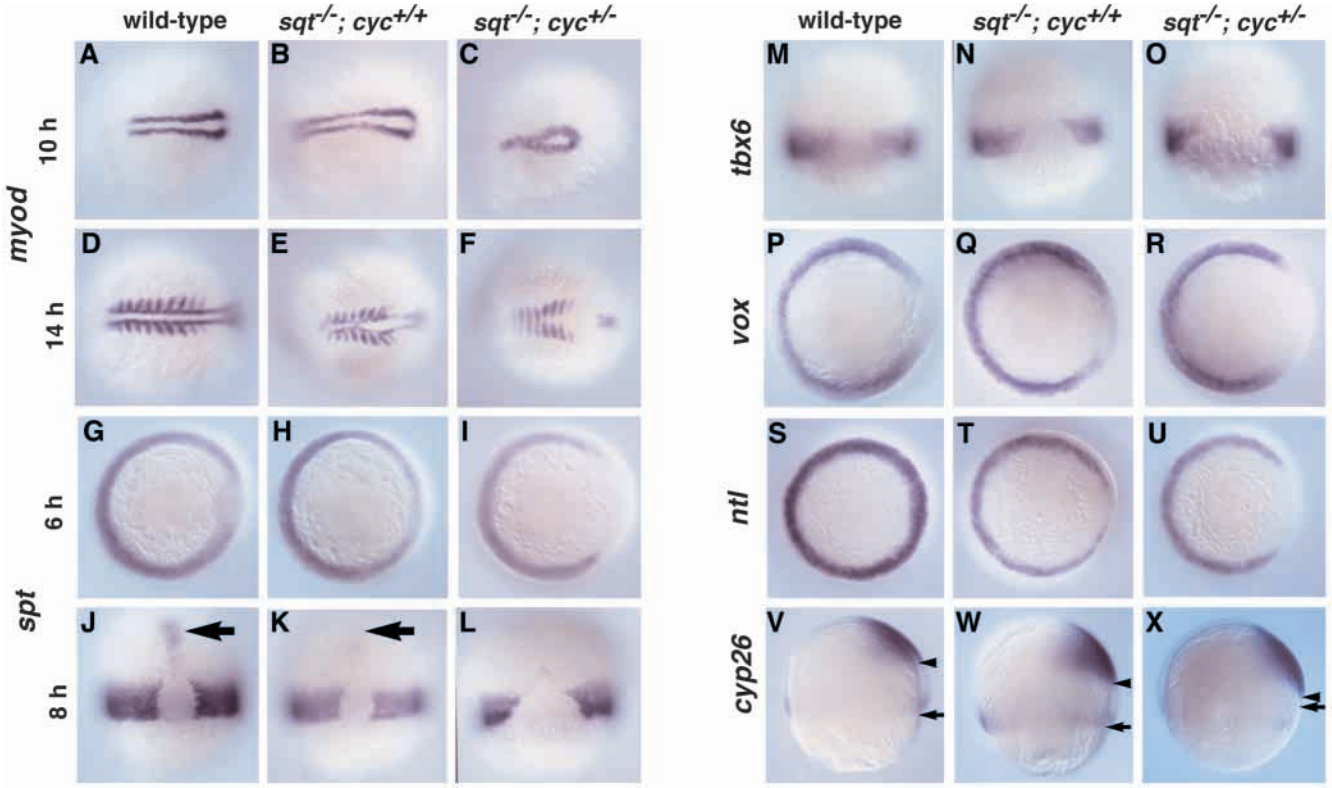

Fig. 6. Analysis of markers for ventrolateral mesoderm and neurectoderm in *sqt*$^{-/-}$; *cyc*$^{+/+}$ and *sqt*$^{-/-}$; *cyc*$^{+/-}$ embryos. The genes, genotypes and stages analyzed are shown. Fusion of paraxial and adaxial *myod* expression domains is apparent in *sqt*$^{-/-}$; *cyc*$^{+/-}$ embryos (C,F). In wild-type, *sqt*$^{-/-}$; *cyc*$^{+/+}$ and *sqt*$^{-/-}$; *cyc*$^{+/-}$ embryos, *spt* (G-L), *tbx6* (M-O) and *vox* (P-R) are each strongly expressed around the ventrolateral margin. *tbx6* and *vox* are normally excluded from the dorsal margin, and this region of exclusion is expanded in *sqt*$^{-/-}$; *cyc*$^{+/-}$ embryos (O,R). *spt* expression in the prechordal plate (J, arrow), is reduced in *sqt*$^{-/-}$; *cyc*$^{+/+}$ (arrow) and absent in *sqt*$^{-/-}$; *cyc*$^{+/-}$ embryos, while marginal expression is excluded from a larger dorsal sector in *sqt*$^{-/-}$; *cyc*$^{+/-}$ embryos (I,L) than in *sqt*$^{-/-}$; *cyc*$^{+/+}$ or wild-type embryos. *ntl* is also reduced dorsally in *sqt*$^{-/-}$; *cyc*$^{+/+}$ (T) and absent dorsally in *sqt*$^{-/-}$; *cyc*$^{+/-}$ (U) embryos. (V-X) Expression of neural marker *cyp26*. Lateral views, dorsal towards the right. Arrow indicates marginal domain of *cyp26* expression, arrowheads indicate vegetal extent of neural domain. The neural expression is shifted slightly towards the margin in *sqt*$^{-/-}$; *cyc*$^{+/+}$ embryos (W), and more dramatically in *sqt*$^{-/-}$; *cyc*$^{+/-}$ embryos (X). In X, the dorsal marginal domain of *cyp26* expression is located at a more animal position than the ventrolateral marginal domain, apparently because of abnormal morphogenetic movements of dorsal cells in *sqt*$^{-/-}$; *cyc*$^{+/-}$ embryos. Dorsal views with anterior towards the left (A-F), animal views with dorsal to the right (G-I,P-R,S-U), dorsal views with animal pole upwards (J-O) and lateral views with animal pole upwards (V-X). The genotypes of all embryos shown were determined by PCR after photography.

trunk notochord, much as they did in wild type (Fig. 7; Fig. 8A″,B″, arrows). In contrast to dorsal marginal cells, the morphogenetic program of cells on the ventrolateral margin appeared normal in *sqt*$^{-/-}$; *cyc*$^{+/-}$ embryos (Fig. 8D, n=33 wild-type and 3 *sqt*$^{-/-}$; *cyc*$^{+/-}$ embryos).

β-catenin activates dorsal expression of *sqt* and *cyc*

The pronounced reduction of dorsal but not ventrolateral mesendoderm in *sqt*$^{-/-}$; *cyc*$^{+/-}$ mutants correlates with the elevated expression of both *sqt* and *cyc* at the dorsal margin (Erter et al., 1998; Feldman et al., 1998; Rebagliati et al., 1998a; Sampath et al., 1998). To understand how the asymmetry of *sqt* and *cyc* expression is generated, we asked if *cyc* is controlled by the maternal dorsal determinant β-catenin, which has been implicated as a regulator of *sqt* and *Xenopus xnr-1* (Hyde and Old, 2000; Shimizu et al., 2000). *β-catenin* mRNA overexpression induced expanded or ectopic *cyc* expression at 6 h in about half (32/60) of injected wild-type embryos (Fig. 9A), similar to the fraction of injected embryos (12/18) with ectopic or expanded *gsc* expression at 5 h (Fig. 9G). Although *β-catenin* did not affect *cyc* expression prior to 6 h (Fig. 9C-F), it induced ectopic or expanded *sqt* expression at 3.3 h (79/112) (Fig. 9K), as previously reported (Shimizu et al., 2000). *β-catenin* had no effect on *sqt* expression at 5 h (Fig. 9M). Thus, activation of *sqt* and *cyc* by β-catenin follow distinct time courses, suggesting that *sqt* may be a direct target, while *cyc* could be an indirect target of β-catenin, mediated by genes such as *sqt* or *boz* that are induced at earlier stages (Fekany et al., 1999).

Because *squint* expression is rapidly upregulated by *β-catenin*, we asked if it is required for *β-catenin* function. We injected *β-catenin* mRNA into embryos from *sqt*$^{+/-}$ parents and analyzed *gsc* expression at 5 h (40% epiboly). At this stage, *gsc* is reduced to only a few cells in control injected and uninjected *sqt* mutants (Fig. 9J). Although *β-catenin* mRNA can induce mutant secondary axes in the absence of *sqt*, as indicated by extra patches of cells expressing low levels of *gsc* (Fig. 9I, arrow), it cannot induce the high levels of *gsc* typical in wild-type embryos (Fig. 9G) (Kelly et al., 1995; Pelegri and Maischein, 1998). Thus, β-catenin requires *squint* function to induce high levels of dorsal

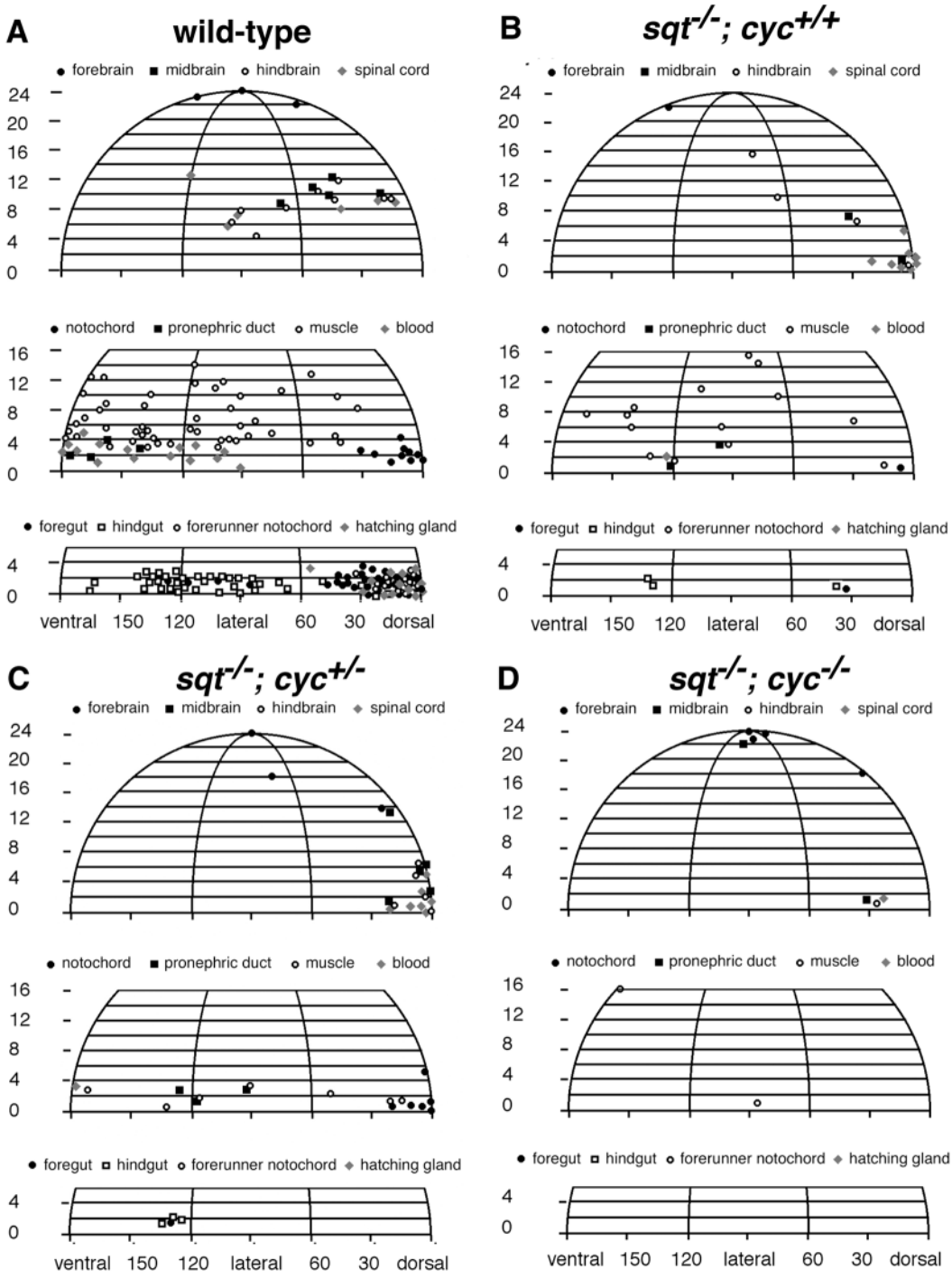

Fig. 7. Fate map of wild-type, $sqt^{-/-}$; $cyc^{+/+}$, $sqt^{-/-}$; $cyc^{+/-}$ and $sqt^{-/-}$; $cyc^{-/-}$ embryos. Positions of clones along the animal-vegetal and dorsoventral axes are depicted on a graphic representation of an embryo, in which each line represents a different row of cells. The '0' line represents cells in contact with the YSL. In the dorsal region, clones generating neural fates arose at least eight cell rows animal to the margin in wild-type (A, top panel). By contrast, $sqt^{-/-}$; $cyc^{+/+}$ (B) and $sqt^{-/-}$; $cyc^{+/-}$ (C) embryos, clones at the dorsal margin produced spinal cord, hindbrain and midbrain. (D) As previously reported, dorsal marginal cells in $sqt^{-/-}$; $cyc^{-/-}$ adopt neural fates. Two ventrolateral clones adopted tail muscle fates. The genotypes of all embryos shown were determined by PCR after photography.

mesodermal gene expression. Nevertheless, β-catenin, acting directly or through other factors, is sufficient to induce low levels of ectopic *gsc* expression in *sqt* mutants.

Consistent with the possibility that β-catenin activates early *sqt* expression, we found that β-catenin protein is localized to the nuclei of presumed dorsal blastomeres prior to 3 h (Fig. 10A-C), when *sqt* transcripts are first detected (Erter et al., 1998; Feldman et al., 1998). These results extend a prior analysis of β-catenin distribution, which reported that β-catenin accumulates in dorsal nuclei at 3.3 h (Schneider et al., 1996). Moreover, we detected nuclear β-catenin in embryos as early as the 128-cell stage (2.25 h) (Fig. 10A), prior to formation of the yolk syncytial layer (YSL), an extra-embryonic structure proposed to have a role in establishing dorsoventral asymmetry in the overlying blastoderm (reviewed by Schier and Talbot, 1998). Nuclear β-catenin was detected in only a small fraction (15%, n=3/20, at the 128-cell stage) of the embryos prior to the 1000-cell stage, perhaps because of intermittent accumulation of nuclear β-catenin during rapid cleavage divisions. Although there are no other markers of

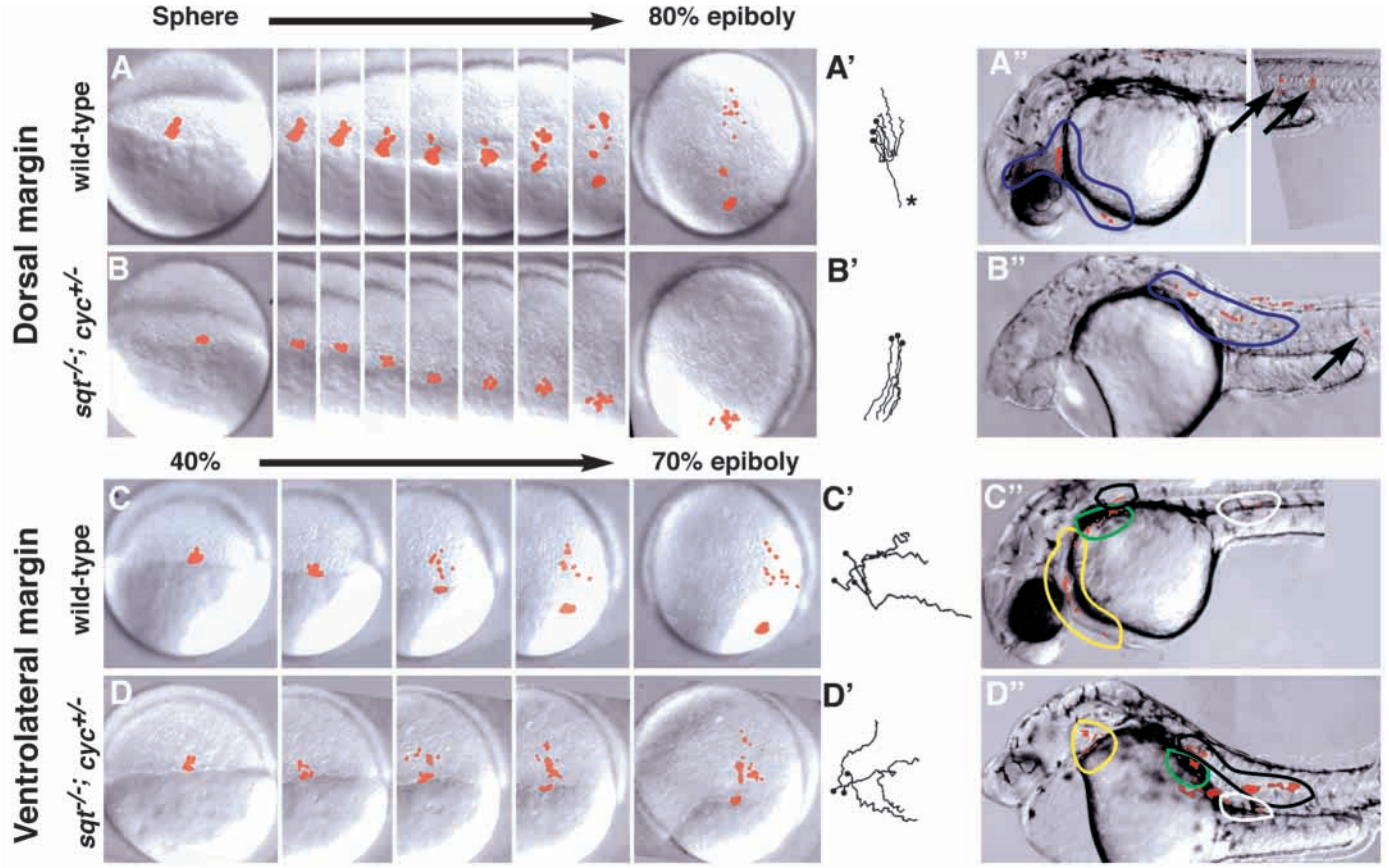

Fig. 8. Aberrant morphogenesis of dorsal clones in *sqt*$^{-/-}$; *cyc*$^{+/-}$ embryos. Morphogenesis and resulting fates of dorsal marginal clones (A,B) and ventrolateral marginal clones (C,D) in wild-type (A,C), and in *sqt*$^{-/-}$; *cyc*$^{+/-}$ embryos (B,D) were examined during the time periods indicated. Tracings of the behavior of individual cells within each clone are shown (A′-D′). Dorsal marginal cells migrate towards the vegetal pole with the movements of epiboly, and begin to involute at the onset of gastrulation at 50% epiboly (A). Some cells do not involute and contribute to the tail (asterisk in A′). In *sqt*$^{-/-}$; *cyc*$^{+/-}$ embryos (B), dorsal marginal cells fail to involute (B′). Whereas the dorsal marginal cells became hatching gland, pharyngeal endoderm and endothelium near the eye in wild type (A″, blue circle), these cells became floorplate in *sqt*$^{-/-}$; *cyc*$^{+/-}$ embryos (B″, blue circles). Arrows in A″ and B″ mark labeled notochord cells. In many *sqt*$^{-/-}$; *cyc*$^{+/-}$ embryos, a region devoid of cells is created at the dorsal midline, possibly generated by the abnormal movements of dorsal marginal cells. By contrast, morphogenetic movements of ventrolateral marginal cells in wild-type (C,C′) and *sqt*$^{-/-}$; *cyc*$^{+/-}$ embryos (D,D′) are indistinguishable, each undergoing the normal movements of epiboly, involution and convergence (Warga and Kimmel, 1990). Labeled cells formed heart endothelium (C″,D″; yellow circles), pronephric duct (C″,D″; white circles), fin bud (C″,D″; green circles), and muscle (C″,D″; black circles) in both wild-type and mutant clones. Other labeled cells (red) are in the EVL. The genotypes of all embryos shown were determined by PCR after photography.

dorsoventral polarity in zebrafish embryos younger than 3 h, the dorsal accumulation of nuclear β-catenin after 3 h has been confirmed by colocalization with dorsal specific genes (Koos and Ho, 1998). Therefore, we presume that β-catenin accumulates in dorsal nuclei prior to 3 h, as it does after 3 h. Our results show that dorsoventral asymmetry is established in the blastoderm before the YSL forms.

DISCUSSION

The role of Nodal signals in mesendodermal patterning

We have examined the role of the zebrafish *nodal*-related genes *squint* and *cyclops* in mesendoderm induction and patterning. Using marker gene analysis and cell tracing, we characterized the fates of dorsal and ventrolateral mesendodermal progenitors in *sqt*$^{-/-}$; *cyc*$^{+/+}$ and *sqt*$^{-/-}$; *cyc*$^{+/-}$ mutants, in which endogenous Nodal signals are reduced but not eliminated. Our data support a role for *nodal*-related genes in patterning marginal blastomeres along the animal-vegetal axis. At the dorsal margin, Nodal signals act to prevent dorsal marginal cells from adopting neurectodermal fates. In wild-type embryos, dorsal marginal cells exclusively form mesendodermal derivatives such as hatching gland, notochord and foregut. By contrast, dorsal marginal cells in *sqt*$^{-/-}$; *cyc*$^{+/+}$ and *sqt*$^{-/-}$; *cyc*$^{+/-}$ mutants often gave rise to neural fates, including spinal cord, hindbrain and midbrain (Fig. 7B,C), and neural marker gene expression was shifted toward the margin (Fig. 6V-X). At the ventrolateral margin, expression of endodermal markers was reduced in *sqt*$^{-/-}$; *cyc*$^{+/+}$ and *sqt*$^{-/-}$; *cyc*$^{+/-}$ mutants (Fig. 5), and muscle precursors were located closer to the margin than in wild-type embryos (Fig. 7). In addition, endoderm was more severely disrupted in *sqt*$^{-/-}$; *cyc*$^{+/-}$ than in *sqt*$^{-/-}$; *cyc*$^{+/+}$ mutants, supporting the proposal that different levels of Nodal signaling establish the mesoderm and endoderm at different positions along the animal-

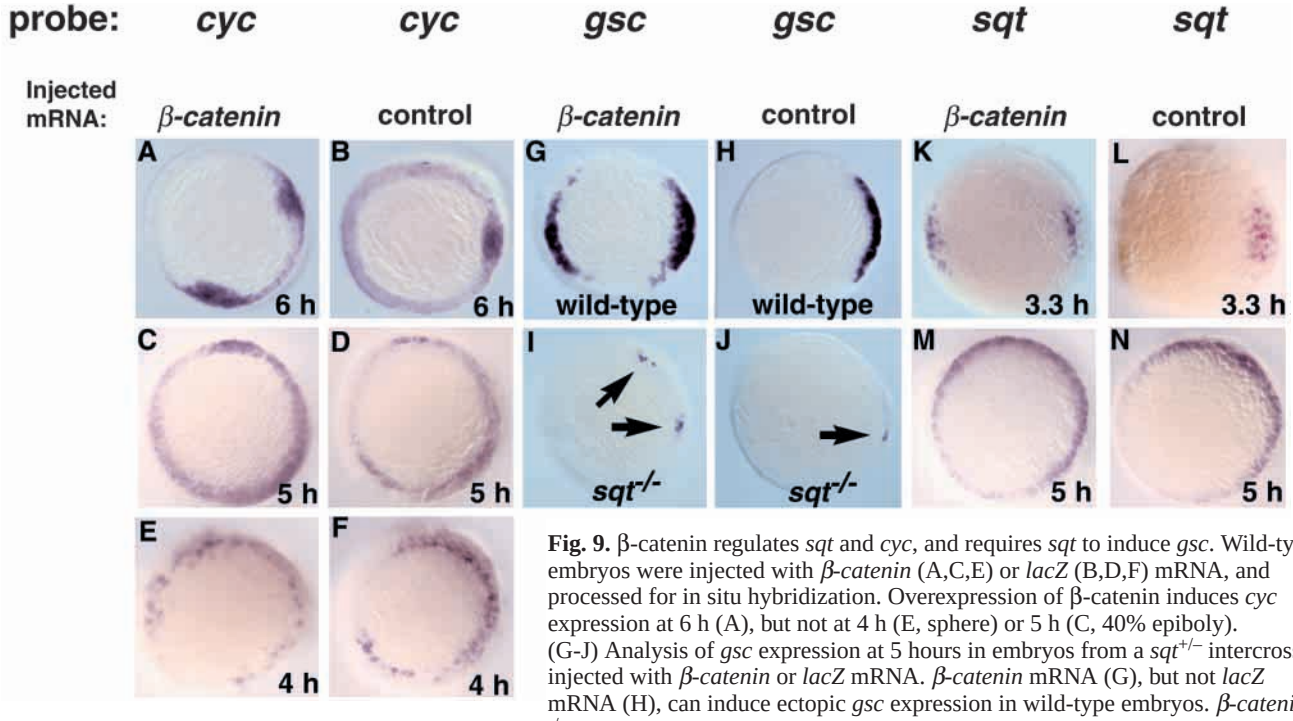

Fig. 9. β-catenin regulates *sqt* and *cyc*, and requires *sqt* to induce *gsc*. Wild-type embryos were injected with *β-catenin* (A,C,E) or *lacZ* (B,D,F) mRNA, and processed for in situ hybridization. Overexpression of β-catenin induces *cyc* expression at 6 h (A), but not at 4 h (E, sphere) or 5 h (C, 40% epiboly). (G-J) Analysis of *gsc* expression at 5 hours in embryos from a $sqt^{+/-}$ intercross injected with *β-catenin* or *lacZ* mRNA. *β-catenin* mRNA (G), but not *lacZ* mRNA (H), can induce ectopic *gsc* expression in wild-type embryos. *β-catenin* mRNA does not induce normal levels of *gsc* expression in $sqt^{-/-}$ mutants (I), but ectopic patches of weak *gsc* are often observed in these embryos, indicating that β-catenin has some activity in *sqt* mutants (arrows, I). β-catenin induces *sqt* expression at 3.3 h (K), but not at 5 h (M, 40% epiboly). Animal views; dorsal towards right when apparent.

vegetal axis (Gritsman et al., 2000; Thisse et al., 2000; Chen and Schier, 2001). The analysis of $sqt^{-/-}$; $cyc^{+/+}$ or $sqt^{-/-}$; $cyc^{+/-}$ mutants extends previous fate mapping studies of Nodal pathway mutants (Feldman et al., 2000; Gritsman et al., 2000; Carmany-Rampey and Schier, 2001) by demonstrating a dosage-sensitive role for Nodal genes in patterning the animal-vegetal axis in dorsal and ventrolateral marginal regions.

Our genetic analyses indicate that mesendodermal progenitors at different positions along the dorsoventral axis have distinct requirements for *nodal*-related genes. In $sqt^{-/-}$; $cyc^{+/-}$ mutants, dorsal axial structures and dorsal expression of early mesendodermal genes such as *gsc*, *axial*, *sox17*, *ntl* and *cyc*, are strongly reduced or eliminated, whereas ventrolateral fates are relatively mildly affected (Figs 2, 5 and 6). This shows that a *nodal* gene dosage sufficient to induce mesendoderm at the ventrolateral margin is insufficient to induce dorsal mesendoderm. In addition, we noted that dorsal, but not ventrolateral, mesendoderm development is quite sensitive to *nodal*-related gene dosage. Dorsal mesendoderm is reduced in $sqt^{-/-}$; $cyc^{+/+}$ mutants, reduced more strongly in $sqt^{-/-}$; $cyc^{+/-}$ mutants, and, as shown in previous studies (Feldman et al., 1998; Gritsman et al., 1999), completely lacking in the absence of Nodal signaling. These differences along the dorsoventral axis are not anticipated by simple models in which Nodal signals act uniformly to induce dorsal and ventrolateral mesendoderm (Fig. 1B).

Differential regulation of *sqt* and *cyc* in dorsal and ventrolateral mesendoderm

Dorsal *sqt* expression is activated by β-catenin (Fig. 9) (Shimizu et al., 2000; Kelly et al., 2000). Previous work (Schneider et al., 1996) has shown that β-catenin localized to dorsal nuclei in the YSL at the 2000-cell stage (3.3 h). We found that β-catenin was detectable in the nuclei of dorsal blastomeres as early as the 128-cell stage (2.25 h) (Fig. 10), prior to formation of the YSL. These results show that dorsoventral asymmetry is established in the blastoderm before the YSL forms. In addition, RNase treatment experiments indicate that RNAs in the YSL are not essential for specification of dorsal identity in overlying blastomeres (Chen and Kimelman, 2000). Taken together, these results establish that β-catenin in dorsal blastomeres specifies dorsal expression of target genes including *sqt* and *boz* (Shimizu et al., 2000; Kelly et al., 2000) and show that the YSL is not required for the initial dorsal identity within the blastoderm. By contrast, the YSL is required for expression of *sqt* and *cyc* in ventrolateral marginal blastomeres (Chen and Kimelman, 2000).

We found that differential regulation of *sqt* and *cyc* expression in dorsal and ventrolateral marginal cells of the late blastula accounts, at least in part, for the differential requirement of *nodal*-related genes along the dorsoventral axis. In the late blastula, *cyc* is expressed in a marginal ring that includes cells at all positions along the dorsoventral axis, but our results show that different mechanisms control *cyc* expression in dorsal and ventrolateral cells. Several observations indicate that *sqt* activates dorsal *cyc* expression in response to the maternal dorsal determinant β-catenin. Overexpression of *β-catenin* induces *sqt* expression soon after the midblastula transition (Fig. 9K) (Shimizu et al., 2000), and nuclear β-catenin protein is present at the correct time and place to directly activate *sqt* expression (Fig. 10). In addition, β-catenin requires *sqt* function for high-level activation of dorsal gene expression (Fig. 9G-J). Dorsal expression of *cyc* in the late blastula is reduced in *sqt* mutants (Fig. 3Q), and overexpression

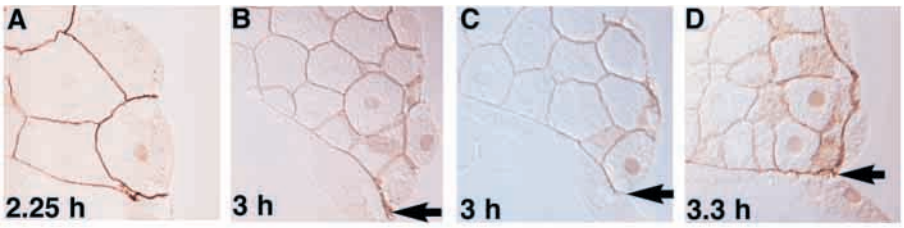

Fig. 10. β-catenin protein is localized in the nucleus at the correct time and place to endogenously regulate *squint* expression. β-catenin protein was detected by immunohistochemistry in whole-mount assays, after which embryos were sectioned. Arrows in B-D indicate boundary between blastomeres and the yolk syncytial layer (YSL). (A) β-catenin in the nucleus of a marginal blastomere at 2.25 h (128-cell stage), the earliest stage detected. (B,C) Nuclear β-catenin is observed in dorsal blastomeres in embryos at 3 h (1000-cell stage), both in the enveloping layer (B,C), and in the deep layer (B). (D) β-catenin accumulates in nuclei of the dorsal YSL at 3.3 h (high stage), but it is also seen in dorsal blastomeres. β-catenin was associated with membranes of blastomeres at all stages examined, consistent with its role in cell adhesion. Dorsal is towards the right.

of *β-catenin* does not activate *cyc* expression until the early gastrula stage (Fig. 9A,C,E). This suggests that β-catenin directly activates *sqt*, which in turn induces dorsal *cyc* expression in the late blastula. At later stages, dorsal *cyc* expression is dependent on an autoregulatory loop, as evidenced by the strong reduction of dorsal *cyc* mRNA in $sqt^{-/-}$; $cyc^{+/-}$ when compared with $sqt^{-/-}$; $cyc^{+/+}$ mutants (Fig. 3) and by previous studies of *cyc* expression in Nodal pathway mutants (Meno et al., 1999; Pogoda et al., 2000; Sirotkin et al., 2000a).

By contrast, ventrolateral expression of *cyc* is induced independently of Nodal signals but requires Nodal activity to achieve normal levels. *cyc* expression is induced normally in ventrolateral marginal cells in $sqt^{-/-}$; $cyc^{+/+}$ embryos, indicating that this expression does not depend on *sqt* function (Fig. 3). In embryos lacking all *nodal* gene function, *cyc* expression is initiated in ventrolateral marginal cells, but does not reach normal levels, whereas dorsal *cyc* expression is not detectable (Meno et al., 1999). These observations indicate that ventrolateral *cyc* expression is induced by as yet unknown factors and maintained at normal levels by an autoregulatory loop. Thus *cyc* expression is controlled differently in dorsal and ventrolateral marginal cells, with dorsal *cyc* expression entirely dependent on *sqt* and *cyc* gene function.

The marked dependence of dorsal, but not ventrolateral, *cyc* expression on Nodal signaling results in a non-uniform reduction of Nodal signals in $sqt^{-/-}$; $cyc^{+/+}$ and $sqt^{-/-}$; $cyc^{+/-}$ mutants. Some dorsal marginal cells in $sqt^{-/-}$; $cyc^{+/+}$ and $sqt^{-/-}$; $cyc^{+/-}$ mutants adopt neural fates because they are exposed to little or no Nodal signals before gastrulation. By contrast, ventrolateral marginal cells in $sqt^{-/-}$; $cyc^{+/+}$ and $sqt^{-/-}$; $cyc^{+/-}$ mutants are exposed to sufficient levels of *cyc* at the late blastula stage to induce ventrolateral mesendoderm. Thus, the role of autoregulation in the reinforcement of dorsal *cyc* expression can explain the severe reduction of dorsal but not ventrolateral fates in $sqt^{-/-}$; $cyc^{+/-}$ mutants.

Experiments in zebrafish, frogs and mice indicate that autoregulation is a conserved feature of the transcriptional control of *nodal*-related genes (this work) (Meno et al., 1999; Hyde and Old, 2000; Osada et al., 2000; Norris et al., 2002). Our results extend this observation by demonstrating that, in zebrafish, cells differ in their sensitivities to the autoregulatory feedback loop depending on their position. *cyc* expression was completely eliminated from dorsal marginal cells in late blastula stage $sqt^{-/-}$; $cyc^{+/+}$ embryos, but was present at reduced levels in ventrolateral marginal cells (Fig. 3P-S). This aspect of the autoregulatory control of *nodal*-related gene expression may also be conserved in other systems, introducing a point of caution in interpreting experiments in which Nodal signaling activity is reduced by genetic methods or by overexpression of Nodal antagonists. It is possible that some cell types are preferentially affected in these experiments.

Dorsoventral patterning of mesendoderm is independent of Nodal signals

Our cell-tracing and gene expression experiments are inconsistent with models proposing that the graded action of Nodal signals patterns the dorsoventral axis (Fig. 1A). Such models predict that dorsal marginal clones should contain fates normally arising at ventrolateral positions, such as muscle, when Nodal signaling is reduced. Rather than muscle or other ventrolateral derivatives, dorsal marginal cells in $sqt^{-/-}$; $cyc^{+/+}$ and $sqt^{-/-}$; $cyc^{+/-}$ mutants often adopt neural fates (Fig. 7B,C). In addition, ventrolateral gene expression was not expanded into dorsal regions (Fig. 6), as would be expected if dorsal marginal cells adopted ventrolateral fates in these mutants. Thus, despite the elevated dorsal requirement for *sqt* and *cyc*, we found no evidence supporting a role for *nodal*-related genes instructing cell fates along the dorsoventral axis. Instead it seems that factors including Chordin, Boz and BMP signals, which are expressed in the absence of Nodal signaling (Gritsman et al., 1999), are able to pattern the dorsoventral axis without an additional instructive role for Nodal signals.

Overlapping and unique functions of *squint* and *cyclops*

Despite the absence of the embryonic shield and dorsal mesendodermal gene expression in all $sqt^{-/-}$ embryos at early stages, many *sqt* mutants have dorsal mesodermal derivatives such as notochord at 24 h, and some survive to adulthood (Table 1). The basis of the variability in the *sqt* mutant phenotype at late stages is not known. Nevertheless, the recovery of dorsal mesendoderm in some *sqt* mutants depends on *cyc* function, because all *sqt*; *cyc* double mutants lack head and trunk mesendodermal derivatives (Fig. 3) (Feldman et al., 1998). Thus, *cyclops* activity can compensate for the loss of *squint* function, either directly or perhaps by activating a parallel pathway that can overcome the loss of *sqt*. This genetic evidence for overlapping functions of the *sqt* and *cyc* genes contrasts with their distinct expression profiles and different activities in misexpression assays (Rebagliati et al., 1998a; Erter et al., 1988).

In misexpression experiments, Cyc acts only over short distances to induce mesodermal gene expression, whereas Sqt acts as a morphogen, directly specifying patterned gene expression over long distances (Chen and Schier, 2001). Thus,

the formation of dorsal mesendoderm in *sqt* mutants demonstrates that Cyc activity can support normal patterning of the late gastrula and viability in the absence of the Sqt morphogen. This suggests that both Sqt and Cyc may act over long distances in their endogenous context, or that the long-range action of a Nodal morphogen is not always essential for viability.

Timing of developmental response to Nodal signals

In light of the different expression profiles of *sqt* and *cyc*, it is interesting that Cyc activity can compensate for loss of *sqt* function. *sqt* expression initiates at the midblastula stage in dorsal marginal cells, while *cyc* transcripts first appear in the late blastula in dorsal and ventral marginal cells. In wild-type embryos, *cyc* expression accumulates to high levels in involuting axial mesoderm, but this expression is reduced and delayed in *sqt* mutants (Fig. 3). Expression of dorsal mesendodermal markers closely follows *cyc* expression in $sqt^{-/-}$; $cyc^{+/+}$ embryos (Fig. 4). For example, *gsc* expression is nearly absent in the late blastula, when *cyc* mRNA is greatly reduced in the dorsal marginal region of these embryos. *gsc* transcripts begin to accumulate at the onset of gastrulation, when *cyc* expression begins to increase at the dorsal midline. Thus, late exposure of dorsal marginal cells to Nodal signals is sufficient for them to adopt dorsal mesendodermal fates. Conversely, dorsal mesendoderm in $sqt^{+/+}$; $cyc^{-/-}$ embryos is induced entirely by *sqt* function and *sqt* expression in these mutants is mostly gone by the beginning of gastrulation (Fig. 3). Thus, exposure of dorsal marginal cells to *sqt* function before gastrulation, or *cyc* function after gastrulation has initiated, is sufficient to specify dorsal mesendoderm. This suggests that the timing of the response to Nodal signaling is not a crucial factor in the specification of dorsal mesendoderm in zebrafish.

We thank David Kimelman, Ariel Ruiz i Altaba, Howie Sirotkin, Ian Woods and Heather Stickney for critical comments on the manuscript; Peter Hausen for supplying β-catenin antibodies; Michele Mittman and Melissa Martin for fish care; and members of our laboratories for helpful discussions. This work was supported by NIH grants GM57825 (W.S.T.), GM56211 (A.F.S.) and GM58513 (D.A.K.). A.F.S. is a Scholar of the McKnight Endowment Fund for Neuroscience, a Irma T. Hirschl Trust Career Scientist and an Established Investigator of the American Heart Association. W.S.T. and D.A.K. were supported by the Pew Scholars Program in the Biomedical Sciences.

REFERENCES

Agius, E., Oelgeschlager, M., Wessely, O., Kemp, C. and de Robertis, E. M. (2000). Endodermal Nodal-related signals and mesoderm induction in Xenopus. *Development* **127**, 1173-1183.

Alexander, J. and Stainier, D. Y. (1999). A molecular pathway leading to endoderm formation in zebrafish. *Curr. Biol.* **9**, 1147-1157.

Bisgrove, B. W., Essner, J. J. and Yost, H. J. (1999). Regulation of midline development by antagonism of lefty and nodal signaling. *Development* **126**, 3253-3262.

Carmany-Rampey, A. and Schier, A. F. (2001). Single-cell internalization during zebrafish gastrulation. *Curr. Biol.* **11**, 1261-1265.

Chen, S.-R. and Kimelman, D. (2000). The role of the yolk syncytial layer in germ layer patterning in zebrafish. *Development* **127**, 4681-4689.

Chen, Y. and Schier, A. F. (2001). The zebrafish Nodal signal Squint functions as a morphogen. *Nature* **411**, 607-610.

Christian, J. L., Olson, D. J. and Moon, R. T. (1992). Xwnt-8 modifies the character of mesoderm induced by bFGF in isolated Xenopus ectoderm. *EMBO J.* **11**, 33-41.

Clements, D., Friday, R. V. and Woodland, H. R. (1999). Mode of action of VegT in mesoderm and endoderm formation. *Development* **126**, 4903-4911.

Conlon, F. L., Lyons, K. M., Takaesu, N., Barth, K. S., Kispert, A., Herrmann, B. and Robertson, E. J. (1994). A primary requirement for nodal in the formation and maintenance of the primitive streak in the mouse. *Development* **120**, 1919-1928.

Cooper, M. S. and D'Amico, L. A. (1996). A cluster of noninvoluting endocytic cells at the margin of the zebrafish blastoderm marks the site of embryonic shield formation. *Dev. Biol.* **180**, 184-198.

Crease, D. J., Dyson, S. and Gurdon, J. B. (1998). Cooperation between the activin and Wnt pathways in the spatial control of organizer gene expression. *Proc. Natl. Acad. Sci. USA* **95**, 4398-4403.

De Robertis, E. M., Larrain, J., Oelgeschlager, M. and Wessely, O. (2000). The establishment of Spemann's organizer and patterning of the vertebrate embryo. *Nat. Rev. Genet.* **1**, 171-181.

Erter, C. E., Solnica-Krezel, L. and Wright, C. V. E. (1998). Zebrafish nodal-related 2 encodes an early mesendodermal inducer signaling from the extraembryonic yolk syncytial layer. *Dev. Biol.* **204**, 361-372.

Faure, S., Lee, M. A., Keller, T., ten Dijke, P. and Whitman, M. (2000). Endogenous patterns of TGFbeta superfamily signaling during early Xenopus development. *Development* **127**, 2917-2931.

Fekany, K., Yamanaka, Y., Leung, T., Sirotkin, H. I., Topczewski, J., Gates, M. A., Hibi, M., Renucci, A., Stemple, D., Radbill, A. et al. (1999). The zebrafish *bozozok* locus encodes Dharma, a homeodomain protein essential for induction of gastrula organizer and dorsoanterior embryonic structures. *Development* **126**, 1427-1438.

Feldman, B., Gates, M. A., Egan, E. S., Dougan, S. T., Rennebeck, G., Sirotkin, H. I., Schier, A. F. and Talbot, W. S. (1998). Zebrafish organizer development and germ-layer formation require nodal- related signals. *Nature* **395**, 181-185.

Feldman, B., Dougan, S. T., Schier, A. F. and Talbot, W. S. (2000). Nodal-related signals establish mesendodermal fate and trunk neural identity in zebrafish. *Curr. Biol.* **10**, 531-534.

Gates, M. A., Kim, L., Egan, E. S., Cardozo, T., Sirotkin, H. I., Dougan, S. T., Lashkari, D., Abagyan, R., Schier, A. F. and Talbot, W. S. (1999). A genetic linkage map for zebrafish: comparative analysis and localization of genes and expressed sequences. *Genome Res.* **9**, 334-347.

Green, J. B., New, H. V. and Smith, J. C. (1992). Responses of embryonic Xenopus cells to activin and FGF are separated by multiple dose thresholds and correspond to distinct axes of the mesoderm. *Cell* **71**, 731-739.

Griffin, K. J., Amacher, S. L., Kimmel, C. B. and Kimelman, D. (1998). Molecular identification of spadetail: regulation of zebrafish trunk and tail mesoderm formation by T-box genes. *Development* **125**, 3379-3388.

Gritsman, K., Zhang, J., Cheng, S., Heckscher, E., Talbot, W. S. and Schier, A. F. (1999). The EGF-CFC protein one-eyed pinhead is essential for nodal signaling. *Cell* **97**, 121-132.

Gritsman, K., Talbot, W. S. and Schier, A. F. (2000). Nodal signaling patterns the organizer. *Development* **127**, 921-932.

Harland, R. and Gerhart, J. (1997). Formation and function of Spemann's organizer. *Annu. Rev. Cell Dev. Biol.* **13**, 611-667.

Hatta, K., Kimmel, C. B., Ho, R. K. and Walker, C. (1991). The cyclops mutation blocks specification of the floor plate of the zebrafish central nervous system. *Nature* **350**, 339-341.

Heasman, J. (1997). Patterning the *Xenopus* blastula. *Development* **124**, 4179-4191.

Heisenberg, C. P. and Nüsslein-Volhard, C. (1997). The function of *silberblick* in the positioning of the eye anlage in the zebrafish embryo. *Dev. Biol.* **184**, 85-94.

Hug, B., Walter, V. and Grunwald, D. J. (1997). *tbx6*, a *Brachyury*-related gene expressed by ventral mesendodermal precursors in the zebrafish embryo. *Dev. Biol.* **183**, 61-73.

Hyde, C. E. and Old, R. W. (2000). Regulation of the early expression of the Xenopus nodal-related 1 gene, Xnr1. *Development* **127**, 1221-1229.

Jones, C. M., Kuehn, M. R., Hogan, B. L., Smith, J. C. and Wright, C. V. E. (1995). Nodal-related signals induce axial mesoderm and dorsalize mesoderm during gastrulation. *Development* **121**, 3651-2662.

Joseph, E. M. and Melton, D. A. (1997). Xnr4: a Xenopus nodal-related gene expressed in the Spemann organizer. *Dev. Biol.* **184**, 367-372.

Kawahara, A., Wilm, T., Solnica-Krezel, L. and Dawid, I. B. (2000). Antagonistic role of *vega1* and *bozozok*/*dharma* homeobox genes in organizer formation. *Proc. Natl. Acad. Sci. USA* **97**, 12121-12126.

Kelly, G. M., Erezyilmaz, D. F. and Moon, R. T. (1995). Induction of a secondary embryonic axis in zebrafish occurs following the overexpression of beta-catenin. *Mech. Dev.* **53**, 261-273.

Kelly, C., Chin, A. J., Leatherman, J. L., Kozlowski, D. J. and Weinberg, E. S. (2000). Maternally controlled β-catenin-mediated signaling is required for organizer formation in the zebrafish. *Development* **127**, 3899-3911.

Kimelman, D., Christian, J. L. and Moon, R. T. (1992). Synergistic principles of development: overlapping patterning systems in Xenopus mesoderm induction. *Development* **116**, 1-9.

Kimelman, D. and Griffin, K. J. (2000). Vertebrate mesendoderm induction and patterning. *Curr. Opin. Genet. Dev.* **10**, 350-356.

Kimmel, C. B., Ballard, W. W., Kimmel, S. R., Ullmann, B. and Schilling, T. F. (1995). Stages of embryonic development of the zebrafish. *Dev. Dyn.* **203**, 253-310.

Kimmel, C. B., Warga, R. M. and Schilling, T. F. (1990). Origin and organization of the zebrafish fate map. *Development* **108**, 581-594.

Koos, D. S. and Ho, R. K. (1998). The *nieuwkoid* gene characterizes and mediates a Nieuwkoop-center-like activity in the zebrafish. *Curr. Biol.* **8**, 1199-1206.

Kudoh, T., Tsang, M., Hukriede, N. A., Chen, X., Dedekian, M., Clarke, C. J., Kiang, A., Schultz, S., Epstein, J. A., Toyama, R. and Dawid, I. B. (2001). A gene expression screen in zebrafish embryogenesis. *Genome Res.* **11**, 1979-1987.

Lee, M. A., Heasman, J. and Whitman, M. (2001). Timing of endogenous activin-like signals and regional specification of the Xenopus embryo. *Development* **128**, 2939-2952.

McDowell, N. and Gurdon, J. B. (1999). Activin as a morphogen in Xenopus mesoderm induction. *Semin. Cell Dev. Biol.* **10**, 311-317.

Melby, A. E., Warga, R. M. and Kimmel, C. B. (1996). Specification of cell fates at the dorsal margin of the zebrafish gastrula. *Development* **122**, 2225-2237.

Melby, A. E., Beach, C., Mullins, M. and Kimelman, D. (2000). Patterning the early zebrafish by the opposing actions of bozozok and vox/vent. *Dev. Biol.* **224**, 275-285.

Meno, C., Gritsman, K., Ohishi, S., Ohfuji, Y., Heckscher, E., Mochida, K., Shimono, A., Kondoh, H., Talbot, W. S., Robertson, E. J. et al. (1999). Mouse Lefty2 and zebrafish antivin are feedback inhibitors of nodal signaling during vertebrate gastrulation. *Mol. Cell* **4**, 287-298.

Moon, R. T. and Kimelman, D. (1998). From cortical rotation to organizer gene expression: toward a molecular explanation of axis specification in Xenopus. *BioEssays* **20**, 536-545.

Norris, D. P., Brennan, J., Bikoff, E. K. and Robertson, E. J. (2002). The Foxh1-dependent autoregulatory enhancer controls the level of Nodal signals in the mouse embryo. *Development* **129**, 3455-3468.

Osada, S. I., Saijoh, Y., Frisch, A., Yeo, C. Y., Adachi, H., Watanabe, M., Whitman, M., Hamada, H. and Wright, C. V. (2000). Activin/nodal responsiveness and asymmetric expression of a Xenopus nodal-related gene converge on a FAST-regulated module in intron 1. *Development* **127**, 2503-2514.

Pelegri, F. and Maischein, H. M. (1998). Function of zebrafish beta-catenin and TCF-3 in dorsoventral patterning. *Mech. Dev.* **77**, 63-74.

Pogoda, H. M., Solnica-Krezel, L., Driever, W. and Meyer, D. (2000). The zebrafish forkhead transcription factor FoxH1/Fast1 is a modulator of nodal signaling required for organizer formation. *Curr. Biol.* **10**, 1041-1049.

Rebagliati, M. R., Toyama, R., Fricke, C., Haffter, P. and Dawid, I. B. (1998a). Zebrafish nodal-related genes are implicated in axial patterning and establishing left-right asymmetry. *Dev. Biol.* **199**, 261-272.

Rebagliati, M. R., Toyama, R., Haffter, P. and Dawid, I. B. (1998b). cyclops encodes a nodal-related factor involved in midline signaling. *Proc. Natl. Acad. Sci. USA* **95**, 9932-9937.

Ruiz i Altaba, A. and Melton, D. A. (1989). Interaction between peptide growth factors and homoeobox genes in the establishment of antero-posterior polarity in frog embryos. *Nature* **341**, 33-38.

Sampath, K., Rubinstein, A. L., Cheng, A. M., Liang, J. O., Fekany, K., Solnica-Krezel, L., Korzh, V., Halpern, M. E. and Wright, C. V. E. (1998). Induction of the zebrafish ventral brain and floorplate requires cyclops/nodal signalling. *Nature* **395**, 185-189.

Schier, A. F. (2001). Axis formation and patterning in zebrafish. *Curr. Opin. Genet. Dev.* **11**, 393-404.

Schier, A. F. and Shen, M. M. (2000). Nodal signalling in vertebrate development. *Nature* **403**, 385-389.

Schier, A. F. and Talbot, W. S. (1998). The zebrafish organizer. *Curr. Opin. Genet. Dev.* **8**, 464-471.

Schier, A. F. and Talbot, W. S. (2001). Nodal signaling and the zebrafish organizer. *Int. J. Dev. Biol.* **45**, 289-297.

Schier, A. F., Neuhauss, S. C., Helde, K. A., Talbot, W. S. and Driever, W. (1997). The *one-eyed pinhead* gene functions in mesoderm and endoderm formation in zebrafish and interacts with *no tail*. *Development* **124**, 327-342.

Schneider, S., Steinbeisser, H., Warga, R. M. and Hausen, P. (1996). Beta-catenin translocation into nuclei demarcates the dorsalizing centers in frog and fish embryos. *Mech. Dev.* **57**, 191-198.

Schohl, A. and Fagotto, F. (2002). Beta-catenin, MAPK and SMAD signaling during early *Xenopus* development. *Development* **129**, 37-52.

Schulte-Merker, S., Ho. R. K., Herrmann, B. G. and Nüsslein-Volhard, C. (1992). The protein product of the zebrafish homologue of the mouse T gene is expressed in nuclei of the germ ring and the notochord of the early embryo. *Development* **116**, 1021-1032.

Shimizu, T., Yamanaka, Y., Ryu, S. L., Hashimoto, H., Yabe, T., Hirata, T., Bae, Y. K., Hibi, M. and Hirano, T. (2000). Cooperative roles of Bozozok/Dharma and Nodal-related proteins in the formation of the dorsal organizer in zebrafish. *Mech. Dev.* **91**, 293-303.

Sirotkin, H. I., Gates, M. A., Kelly, P. D., Schier, A. F. and Talbot, W. S. (2000a). Fast1 is required for the development of dorsal axial structures in zebrafish. *Curr. Biol.* **10**, 1051-1054.

Sirotkin, H. I., Dougan, S. T., Schier, A. F. and Talbot, W. S. (2000b). *bozozok* and *squint* act in parallel to specify dorsal mesoderm and anterior neuroectoderm in zebrafish. *Development* **127**, 2583-2592.

Smith, J. C., Yaqoob, M. and Symes, K. (1998). Purification, partial characterization and biological effects of the XTC mesoderm-inducing factor. *Development* **103**, 591-600.

Stachel, S. E., Grunwald, D. J. and Myers, P. Z. (1993). Lithium perturbation and *goosecoid* expression identify a dorsal specification pathway in the pregastrula zebrafish. *Development* **117**, 1261-1274.

Strahle, U., Blader, P., Henrique, D. and Ingham, P. W. (1993). Axial, a zebrafish gene expressed along the developing body axis, shows altered expression in cyclops mutant embryos. *Genes Dev.* **7**, 1436-1446.

Takahashi, S., Yokota, C., Takano, K., Tanegashima, K., Onuma, Y., Goto, J. and Asashima, M. (2000). Two novel nodal-related genes initiate early inductive events in Xenopus Nieuwkoop center. *Development* **127**, 5319-5329.

Talbot, W. S., Egan, E. S., Gates, M. A., Walker, C., Ullmann, B., Neuhauss, S. C., Kimmel, C. B. and Postlethwait, J. H. (1998). Genetic analysis of chromosomal rearrangements in the cyclops region of the zebrafish genome. *Genetics* **148**, 373-380.

Thisse, B., Wright, C. V. and Thisse, C. (2000). Activin- and Nodal-related factors control antero-posterior patterning of the zebrafish embryo. *Nature* **403**, 425-428.

Thisse, C., Thisse, B., Halpern, M. E. and Postlethwait, J. H. (1994). Goosecoid expression in neurectoderm and mesendoderm is disrupted in zebrafish cyclops gastrulas. *Dev. Biol.* **164**, 420-429.

Thisse, C. and Thisse, B. (1999). Antivin, a novel and divergent member of the TGFβ superfamily, negatively regulates mesoderm induction. *Development* **126**, 229-240.

Varlet, I., Collignon, J. and Robertson, E. J. (1997). *nodal* expression in the primitive endoderm is required for specification of the anterior axis during mouse gastrulation. *Development* **124**, 1033-1044.

Warga, R. M. and Kimmel, C. B. (1990). Cell movements during epiboly and gastrulation in zebrafish. *Development* **108**, 569-580.

Warga, R. M. and Nüsslein-Volhard, C. (1998). spadetail-dependent cell compaction of the dorsal zebrafish blastula. *Dev. Biol.* **203**, 116-121.

Warga, R. M. and Nüsslein-Volhard, C. (1999). Origin and development of the zebrafish endoderm. *Development* **126**, 827-838.

Watabe, T., Kim, S., Candia, A., Rothbacher, U., Hashimoto, C., Inoue, K. and Cho, K. W. (1995). Molecular mechanisms of Spemann's organizer formation: conserved growth factor synergy between Xenopus and mouse. *Genes Dev.* **9**, 3038-3050.

Weinberg, E. S., Allende, M. L., Kelly, C. S., Abdelhamid, A., Murakami, T., Andermann, P., Doerre, O. G., Grunwald, D. J. and Riggleman, B. (1996). Developmental regulation of zebrafish MyoD in wild-type, no tail and spadetail embryos. *Development* **122**, 271-280.

White, J. A., Guo, Y. D., Batez, K., Beckett-Jones, B., Bonasoro, J., Hsu, K. E., Dilworth, F. J., Jones, G. and Petkovich, M. (1996). Identification of the retinoic acid-inducible all-trans-retinoic acid 4-hydroxylase. *J. Biol. Chem.* **271**, 29922-29927.

Whitman, M. (2001). Nodal signaling in early vertebrate embryos: themes and variations. *Dev. Cell* **1**, 605-617.